AFRL-ML-WP-TR-1998-4120

HALON REPLACEMENT FOR AIRCRAFT FIRE SUPPRESSION SYSTEMS

PETER D. HAALAND
JOHN H. HUNTINGTON

HUNTINGTON RESEARCH AND ENGINEERING
P.O. BOX 90118
SAN JOSE CA 95109

JUNE 1998

THIS IS A SMALL BUSINESS INNOVATIVE RESEARCH (SBIR) PHASE II REPORT

FINAL REPORT FOR PERIOD 1 AUGUST 1995 – 1 FEBRUARY 1998

Approved for public release; distribution unlimited

MATERIALS & MANUFACTURING DIRECTORATE
AIR FORCE RESEARCH LABORATORY
AIR FORCE MATERIEL COMMAND
WRIGHT-PATTERSON AIR FORCE BASE, OH 45433-7734

NOTICE

USING GOVERNMENT DRAWINGS, SPECIFICATIONS, OR OTHER DATA INCLUDED IN THIS DOCUMENT FOR ANY PURPOSE OTHER THAN GOVERNMENT PROCUREMENT DOES NOT IN ANY WAY OBLIGATE THE US GOVERNMENT. THE FACT THAT THE GOVERNMENT FORMULATED OR SUPPLIED THE DRAWINGS, SPECIFICATIONS, OR OTHER DATA DOES NOT LICENSE THE HOLDER OR ANY OTHER PERSON OR CORPORATION; OR CONVEY ANY RIGHTS OR PERMISSION TO MANUFACTURE, USE, OR SELL ANY PATENTED INVENTION THAT MAY RELATE TO THEM.

THIS REPORT IS RELEASABLE TO THE NATIONAL TECHNICAL INFORMATION SERVICE (NTIS). AT NTIS, IT WILL BE AVAILABLE TO THE GENERAL PUBLIC, INCLUDING FOREIGN NATIONS.

THIS TECHNICAL REPORT HAS BEEN REVIEWED AND IS APPROVED FOR PUBLICATION.

GREGORY J. CECERE, Project Engineer
Nonstructural Materials Branch
Nonmetallic Materials Division

STEPHEN L. SZARUGA, Acting Chief
Nonstructural Materials Branch
Nonmetallic Materials Division

ROGER D. GRISWOLD, Assistant Chief
Nonmetallic Materials Division
Materials & Manufacturing Directorate

Do not return copies of this report unless contractual obligations or notice on a specific document requires its return.

REPORT DOCUMENTATION PAGE	Form Approved OMB No. 0704-0188

1. AGENCY USE ONLY *(Leave blank)*	2. REPORT DATE	3. REPORT TYPE AND DATES COVERED
	June 1998	Final Report 1 Aug 95 – 1 Feb 98

4. TITLE AND SUBTITLE
HALON REPLACEMENT FOR AIRCRAFT FIRE SUPPRESSION SYSTEMS

5. FUNDING NUMBERS
C F33615-95-C-5045
PE 65502F
PR 3005
TA 05
WU M5

6. AUTHOR(S)
Dr. Peter C. Haaland and Dr. John Huntington

7. PERFORMING ORGANIZATION NAME(S) AND ADDRESS(ES)
Huntington Research and Engineering
P.O. Box 90118
San Jose CA 95109

8. PERFORMING ORGANIZATION REPORT NUMBER
FR4021

9. SPONSORING/MONITORING AGENCY NAME(S) AND ADDRESS(ES)
Materials & Manufacturing Directorate
Air Force Research Laboratory
Air Force Materiel Command
Wright-Patterson Air Force Base, Oh 45433-7734
POC: Gregory J Cecere, AFRL/MLBT, 937-255-2199

10. SPONSORING/MONITORING AGENCY REPORT NUMBER
AFRL-ML-WP-TR-1998-4120

11. SUPPLEMENTARY NOTES

12a. DISTRIBUTION AVAILABILITY STATEMENT
Approved for public release, distribution unlimited.

12b. DISTRIBUTION CODE

13. ABSTRACT *(Maximum 200 words)*

The objective of this program was to demonstrate the effectiveness and to determine the toxicity and associated risks of labile bromine compounds as halon replacements for suppression of engine nacelle and dry-bay fires in military aircraft. Tests performed during this program have shown that labile bromine compounds generally and phosphorous tribromide (PBr3) in particular, are more effective than Halon 1301 for both engine nacelle and dry-bay fire extinguishment and have neither ozone depletion nor global warming potentials. Theoretical electronic structure calculations and experimental chemical kinetics investigations were performed to enhance the understanding of the chemical action of PBr3 fire suppression. Independent toxicity studies supervised by the tri-services toxicology laboratory (AL/OET) at Wright Patterson Air Force Base, determined that PBr3 was neither mutagenic nor toxic to aquatic organisms. Additional data on the toxicological properties of PBr3 were acquired by AL/OET including dermal irritation and acute and subchronic inhalation toxicity. These results formed the basis of their independent risk assessment, which concludes that use of PBr3 as a halon replacement is safe in normally unoccupied spaces such as engine nacelles or dry-bays.

14. SUBJECT TERMS
Halon, halon replacement, fire suppression, nacelle, dry-bay, ozone depletion, PBr3

15. NUMBER OF PAGES
53

16. PRICE CODE

17. SECURITY CLASSIFICATION OF REPORT	18. SECURITY CLASSIFICATION OF THIS PAGE	19. SECURITY CLASSIFICATION OF ABSTRACT	20. LIMITATION OF ABSTRACT
UNCLASSIFIED	UNCLASSIFIED	UNCLASSIFIED	SAR

Standard Form 298 (Rev. 2-89) (EG)
Prescribed by ANSI Std. 239.18
Designed using Perform Pro, WHS/DIOR, Oct 94

Labile Bromine Fire Suppressants

Peter Haaland
John Huntington
Huntington Research and Engineering
P.O. Box 90118
San Jose, CA 95109

Abstract

The objective of this program was to demonstrate the effectiveness and to determine the toxicity and associated risks of labile bromine compounds as Halon replacements for suppression of engine nacelle and dry-bay fires in military aircraft. Tests performed during this program have shown that labile bromine compounds generally, and phosphorous tribromide in particular, are more effective than Halon 1301 for both engine nacelle and dry-bay fire extinguishment and have neither ozone depletion nor global warming potentials. Theoretical electronic structure calculations and experimental chemical kinetics investigations were performed to enhance the understanding of the chemical action of phosphorous tribromide in fire suppression. Independent toxicity studies supervised by the tri-services toxicology laboratory AL/OET determined that phosphorous tribromide was neither mutagenic nor toxic to aquatic organisms. Additional data on the toxicological properties of PBr_3 were acquired by AL/OET including dermal irritation and acute and subchronic inhalation toxicity. These results formed the basis of their independent risk assessment, which concludes that use of PBr_3 as a Halon replacement is safe in normally unoccupied spaces such as engine nacelles or dry-bays.

TABLE OF CONTENTS

TABLE OF CONTENTS	1
LIST OF FIGURES	2
LIST OF TABLES	3
1. Background	4
2. Motivation	6
3. Principles of Experiment Design	7
4. Scientific Approach	10
5. Labile Bromine in PBr_3	10
6. Nacelle Fire Testing	12
7. Dry Bay Fire Suppression	17
8. Theoretical Chemistry	22
8.1. Structure and Energetics of PBr_3 and Related Species	22
8.2 Methodology for structure and energetics	23
8.3 Rates	27
9. Experimental Chemical Kinetics	30
9.1 UV Detection of PBr_3	31
9.2 Hydrolysis of PBr_3	32
9.3 Unimolecular Decomposition	33
9.4 Reactions with Radicals	34
10. Toxicology of PBr_3	36
11. Risk Assessment	37
11.1 Transport properties of PBr_3 vapor	38
11.2 Risk Assessment for Phosphorous Tribromide.	41
11.2.1 Hazard Assessment	42
11.2.2 Exposure Assessment	45
11.2.3 Risk Characterization	48
11.2.4 Risk Assessment Conclusions	49
11.2.5 Risk Assessment References	50
12. Conclusions: Labile Bromine Fire Suppressants	51

LIST OF FIGURES

Figure 1. *Unimolecular lifetimes of PBr_x and CF_3Br as a function of temperature using RRKM theory. Release of bromine atoms by PBr_x is substantially faster than that by Halon 1301.* 11

Figure 2. *Temperature dependent bimolecular rate coefficients (cm^3s^{-1}) for Br abstraction from three PBr_x compounds by hydrogen atoms.* 12

Figure 3 *End-on view of the nacelle simulator burning 10g/second (12 cc/second) of kerosene in a 13 m/s, 3000 cfm airflow.* 13

Figure 4 *Five seconds after fuel flow has been interrupted the fire continues to burn in the flame-holder region. Temperatures up to 800° C have been measured in this region 7 seconds after fuel termination.* 14

Figure 5. *First frame of video (within 33 ms) record following injection of 10cc of PBr_3 by about 1 liter atmosphere of nitrogen through a ruptured foil diaphragm.* 15

Figure 6. *Two frames later (100 ms after injection) there is no evidence of flame and copious unburned fuel in the form of kerosene smoke is visible.* 16

Figure 7. *Thirty frames (one second) following suppressant addition we see no evidence of combustion in the nacelle, even around the flame holder, despite the fact that fuel continues to flow at 10 grams per second.* 16

Figure 8. *Fire in the dry-bay simulator showing 5 meter tongue of flame propelled through the exit wound in the center of the device. Injectors for fuel (center) and extinguishant (right) are also shown.* 18

Figure 9. *Six seconds after the initial fire, combustion continues on surfaces that were wetted by fuel. This burning continues both with and without ventilation by the 140 cfm blower.* 18

Figure 10. *This fire has fully developed before we inject 10 cc of PBr_3 into the bay from the cylinder at the right of the figure.* 19

Figure 11. *One thirtieth of a second (one frame) following injection of PBr_3 we see evidence of suppression in white smoke on the right half of the bay.* 19

Figure 12. *Two frame later, or 100 ms following injection of the suppressant, the extinguishment continues.* 20

Figure 13. *The fire is completely suppressed, with no combustion on the wetted surfaces, only ten frames after injection of 10 cc of PBr_3.* 20

Figure 14. Pressure pulses recorded by a differential transducer for the simulated fuel-tank explosion that results from injection of a 75 cc kerosene spray onto a burning automotive flare in the 0.3 cubic meter dry-bay. A falling signal indicates increasing pressure in the dry-bay. 21

Figure 15.*Ultraviolet absorption cross-section for PBr_3 vapor.* 31

Figure 16*PBr_3 vapor pressure (Torr) between 10 and 30 Celsius on a linear scale. The room-temperature vapor pressure is 2.25 Torr.* 38

Figure 17*Vapor pressure (Torr) of PBr_3 between 0°C and its boiling point at atmospheric pressure.* 39

Figure 18. *Mass of PBr_3 (milligrams) versus time (seconds) in an open weigh boat with a 15.5 cm^2 surface exposed to moderate ventilation at room temperature.* 46

LIST OF TABLES

Table 1: Equilibrium Geometries 22
Table 2. MP2/6-311G(d)//MP2/6-31G(d) Energies 23
Table 3. MP2/6-311G(d)//MP2/6-31G(d) Dissociation Thresholds 23
Table 4. MP2/6-31G(d)[ECP(HW)] Structures used in G2 calculations 25
Table 5. G2(ECP/HW) Energies 26
Table 6. H+HBr System: MP2/6-311+G(d,p) Structures 26
Table 7. H+HBr System: Better-than-G2 Energies 26
Table 8. MP2/6-31G(d)[ECP(HW)] Partition-Function Data 28
Table 9. Partition-Function Data Used for Unimolecular Dissociations, Including Data for Approximate MCSCF Transition-State Structures 29
Table 10. G2[ECP(HW)] Activation Energies for Bimolecular Reactions 30
Table 11. Activation Energies Employed in Unimolecular Reactions 30
Table 12. Data Employed for H + HBr <--> H2 + Br Rates 30

1. Background

The depletion of stratospheric ozone by anthropogenic Halons continues to be an international concern. Scientists at the National Oceanic and Atmospheric Adminstration released the following report on February 19th, 1998:

> SOME OZONE DEPLETING CHEMICALS CONTINUE TO INCREASE IN ATMOSPHERE
>
> Despite a ban on the production of ozone-depleting Halons by developed countries, the compounds continue to increase in the atmosphere according to a new study by the Commerce Department's National Oceanic and Atmospheric Administration. Measurements by scientists at NOAA's Climate Monitoring and Diagnostics Laboratory in Boulder, Colo., indicate that three bromine-containing fire extinguishants, Halons H-1211, H-1301 and H-2402 are still being released into the atmosphere in crucial amounts. The findings are reported in the January 20, 1998 issue of the Journal of Geophysical Research and are the result of a 10-year analysis of air samples from eight remote climate monitoring stations, which were sampled on a biweekly and /or monthly basis, and seven research cruises in the remote ocean. A companion paper, by Wamsley, et al, reporting similar results of measurements from high-altitude aircraft, which calculated total bromine in the lower stratosphere, also appears in the same issue.
>
> Scientists are concerned about the increase in Halons because bromine, an element in the Halons, is 50 times more efficient at depleting ozone in the atmosphere than it's nearest rival, chlorine, a component in chlorofluorocarbons (CFCs), and because the gases last a long time in the atmosphere. "Given the current atmospheric record and the reported amount of Halon produced before the ban on production, emission of one of these compounds could continue for another 40 years," scientist and lead author James Butler said. "These increases are significant and of concern because of the efficiency of bromine in depleting stratospheric ozone and because of the long atmospheric lifetimes of these gases," said Butler. According to Butler, there are as yet no suitable substitutes for all Halon uses, some of which are critical.
>
> The main sources of the compounds are from stockpiles of Halons produced before the ban on production and from developing nations, such as China. In fact, China alone generated almost 90% of the global production of Halon in 1994. Continued increases in production in developing countries are allowed within the Montreal Protocol until the year 2002, at which time they will have to freeze production at the 1995-97 levels. The Montreal Protocol is an international agreement to limit ozone-damaging compounds that was originally signed by the United States and 22 other nations in 1987, and subsequently revised and amended.

Halocarbons that contain bromine atoms have been remarkably successful as fire suppressants. Halon 1301 (CF_3Br), Halon 1211 (CF_2ClBr), and Halon 2402 ($C_2F_4Br_2$) are

widely employed for fire suppression because much larger quantities of unbrominated halocarbons such as CF_4, HCF_3, or C_2F_5H are required to suppress standard fires. The reason for the improved performance of bromine-bearing halocarbons is that bromine atoms are released either by pyrolysis:

$$CF_3Br + \text{heat} \text{ ------> } CF_3 + Br,$$

or by reaction with flame radicals, for example:

$$H + CF_3Br \text{ ------> } HBr + CF_3$$

$$HO + CF_3Br \text{ ------> } HOBr + CF_3.$$

Once released into the flame environment the free bromine catalyzes recombination of combustion intermediates to chemically extinguish the fire. Typical cycles for catalysis of atomic recombination by Br include

Br	+	H	+	N_2	----->	HBr	+ N_2
HBr	+	H			----->	H_2	+ Br
net reaction		H	+	H	----->	H_2	

and

Br	+	O	+	N_2	----->	OBr	+ N_2
OBr	+	O			----->	O_2	+ Br
net reaction		O	+	O	----->	O_2.	

In the course of these reactions the bromine is neither consumed nor produced, so each Br atom can participate in the acceleration of hundreds of millions of recombination events. The peculiar catalytic activity of bromine also applies to stratospheric ozone molecules:

Br	+	O_3	----->	BrO	+	O_2
BrO	+	O_3	----->	Br	+	$2O_2$
net reaction		$2O_3$	----->	$3O_2$.		

The Achilles heel of the bromine-bearing Halons 1301, 2402, and 1211 is their peculiar chemical stability. When released into the troposphere they are neither soluble in water nor

reactive with atmospheric oxidants such as OH. They don't adsorb efficiently to surfaces either. After about 13 months, they are transported by atmospheric motion and diffusion to the stratosphere, where they remain for about 11 years. The short-wavelength ultraviolet light of the sun at these altitudes photolyzes the Halons to release free bromine atoms, where they may catalyze the conversion of ozone to oxygen and shift the dynamical balance to lower steady-state ozone concentrations. Other atmospheric chemical and fluid dynamics can exaggerate the catalytic shift. For example, the presence of water vapor and NO_x in the mid-latitude stratosphere buffers free bromine and chlorine by forming nitrates. The cold, desiccated atmosphere over the Antarctic polar vortex in the Austral winter freezes out the nitric oxide buffers and permits the dramatic ozone depletion popularly known as the ozone hole to form as the sun rises over Antarctica in the Austral spring.

The realization that chemically stable chloro- and bromo-carbon gases cause anthropogenic damage to the atmosphere precipitated international treaties to constrain the production and use of these compounds. At the same time their combination of potency and chemical stability made Halons irresistible to the aviation community for suppression of fires aboard aircraft. The objective of the work described in this report was to identify and evaluate alternative methods for chemically quenching combustion by delivering bromine atoms to a flame without harming stratospheric ozone.

2. Motivation

Fire suppression is caused by varied combinations of four basic mechanisms:

(1) displacement of oxidizer (e.g. CO_2 or N_2 displacing O_2).

(2) lowering of flame temperature by enthalpy extraction (e.g., a phase change of H_2O from liquid to gaseous)

(3) disruption of flame chemistry by stoichiometric or catalytic reactions.

(4) removal of fuel from the combustion environment.

There is ample evidence in the fire suppression literature that Halon 1301, CF_3Br, is more potent than its perfluorinated analog, CF_4. We inferred that this difference was due to the catalytic reactions of bromine atoms that are released when Halon 1301 is pyrolyzed in a flame. The catalytic efficiency of bromine atoms in ozone depletion is by now well-established. Yet the strong C-Br bond in Halon 1301 (~ 270 kJ/mole) makes the molecule unreactive with water, OH, or other tropospheric species, allowing it to be transported by diffusion and convection to the stratosphere. There it is photolyzed by solar ultraviolet light to produce halogen atoms that deplete the ozone layer. We reasoned that a compound with weaker bonds to bromine would be more potent than Halons for suppressing fires and, for the same reason, unable to reach the stratosphere.

3. Principles of Experiment Design

At the time this work was proposed we assumed that the Air Force would prefer that the effectiveness of PBr_3 extinguishers be demonstrated in existing Air Force facilities designed to simulate engine nacelle and dry bay fires. We had a verbal commitment that time for our tests would be provided in the engine nacelle fire test fixture at the Air Force Flight Dynamics Directorate Survivability Branch (WL/FIVS). In spite of our best efforts, it proved impossible to schedule time on that facility. We therefore used the travel and subsistence budget to build our own full-scale facilities. Since we had the freedom to design these facilities, we could apply established principles of experiment design. The design of the Air Force engine nacelle facility was not made available to us, however limited information has since been released in Air Force Technical Reports.

We have observed a very wide range of effectiveness and efficiency in doing experimental work. In our experience the most important independent variable in an experimental program is the experimenter himself. Valuable time is wasted and insecure conclusions are

reached as consequences of inappropriately posing the questions to be resolved, and of designing the experimental conditions in such a way as to obscure, rather than clarify, the key questions. The following quotation is from *An Introduction to Scientific Research* by E. Bright Wilson, Jr. (McGraw-Hill, New York, 1952). Wilson, who was for many years the most respected researcher in Harvard's Department of Chemistry, wrote:

> Before planning actual experiments, the investigator should obviously have a good basic understanding of the nature of the problem and of any relevant theory associated with it. Even a very imperfect theory will often provide existence theorems, limiting values, etc., of considerable utility in guiding experiments. In some cases it is possible to set up a single experiment whose outcome largely determines the fate of a given hypothesis. This is called a "critical experiment". It is rather poor policy to carry out an experiment without a clear-cut idea in advance of just what is being tested.

To this sensible policy we must add our own observation that the commonest way to confound the interpretation of tests is to confuse dependent with independent variables in the experimental design. Fire extinguishment tests require dealing with a statistical problem, since the fluid dynamics of the flame inherently includes large fluctuations. Transient conditions within a flame can introduce non-reproducible sources of reignition. Both the physico-chemical and fluid dynamical boundary conditions strongly influence the outcome of a particular extinguishment test. Accordingly, we chose to do full-scale, realistic tests, such as are conducted by Underwriters Laboratories, Inc., in certifying fire extinguishers. The purpose of our tests was:

> *to provide a means of defining the efficacy of extinguishants under realistic conditions simulating jet engine nacelle and dry bay fires.*

We therefore designed engine nacelle experiments that looked quite different from those the Air Force had been doing. The test results reported by the Air Force in Halon Replacement Program for Aviation: Aircraft Engine Nacelle Application Phase I (WL-TR-95-3077) claimed that "surface temperature", "fuel temperature", and "preburn time", which were independently controlled variables in their tests, were more important variables than

"extinquishant". The conclusion on the importance of surface temperature was made on the basis of measurements at only two temperatures, one being quite high. It should not be surprising that surfaces held above the either the flash point or the ignition temperature will reignite the fuel fire, since the fuel is present as both liquid and vapor. Indeed all three variables, "surface temperature", "fuel temperature", and "preburn time", affect the probability of reignition, so experimental principles dictate that they be allowed to assume realistic values by means of experimental simulation, rather than be independently controlled. The Air Force tests confounded the question of extinguishant efficacy, making the interpretation of the experiments more difficult than one would prefer.

Our nacelle simulators used fixed flame holders to support a flame that cannot easily be put out. Surface temperatures were strictly dependent upon the flame and preburn time, which were not varied. Nor was the rate of fuel flow or fuel type. The independent variables in our tests were:

- Extinguishant composition
- Extinguishant quantity
- Rate of extinguishant addition
- Propellant gas
- Extinguisher placement

The dry bay facility, in contrast to the nacelle facility, was patterned after an Air Force drawing, with the exception that one full side was made of transparent material to facilitate direct viewing of the transient flame conditions. The dry bay tests proved to be straightforward. We injected a fuel spray with a puff of air or nitrogen in a reproducible manner, and provided a consistent, pyrotechnic ignition source within the bay. Independently controlled variables were:

- Fuel quantity
- PBr_3 extinguishant quantity
- Extinguisher delay
- Extinguisher location

4. Scientific Approach

A series of chemical compounds with labile (weakly bound) bromine were screened during the phase I SBIR contract with the Wright Laboratory Materials Directorate. Phosphorous tribromide, PBr_3, a dense (2.8 g/cc) liquid brominating agent, was selected as a promising candidate for full-scale testing on engine nacelle and dry-bay fires. The vapor of this material reacts rapidly with water to give hydrobromic and phosphonic acids, both of which are very soluble in water:

$$PBr_3 + 3\,H_2O \rightarrow H_3PO_3 + 3\,HBr \qquad 2 \times 10^{-17} < k < 6 \times 10^{-17} \text{ cc/s.}$$

The reaction of liquid PBr_3 with liquid water is also immediate, with all of the phosphonic acid product and some of the HBr remaining dissolved in water. The bounds on the gas-phase reaction rate imply a lifetime for the vapor in 50% relative humidity air at one atmosphere and room temperature of about 80 milliseconds. It should be noted that PBr_3 also reacts rapidly with OH radicals that are present in the troposphere, leading to a lifetime of several hours by this decomposition channel. In either case, the lifetime of PBr_3 is more than three orders of magnitude less than the thirteen month transport time for this material to the stratosphere. It therefore has **zero ozone depletion potential and zero global warming potential.**

The material's low vapor pressure and rapid reaction with water to produce mild acids also constrain its toxicological impact. In the unlikely event that PBr_3 vapor survives hydrolysis in the atmosphere, its instantaneous hydrolysis on mucosa precludes its transport to the heart muscle or central nervous system such as are shown to occur with chemically 'inert' Halon replacements such as CF_3I.

5. Labile Bromine in PBr_3

In order to estimate the fate of PBr_3 in a flame we have computed the rates for unimolecular thermal decomposition of PBr_3, PBr_2, and PBr in collaboration with Drs. McKoy and

Winstead of the California Institute of Technology. A detailed description of these calculations is provided in the section titled Theoretical Chemistry. The potential energy surface for the molecules using *ab initio* electronic structure theory provide estimates of the energetics and partition functions for the equilibrium and transition state conformations that are used to calculate the temperature-dependent unimolecular decomposition rates. The lifetime of these PBr_x molecules at the flame temperatures measured in our nacelle experiments is tens of microseconds (Figure1), much shorter than the characteristic diffusion and residence times of the combusting gases. This means that Br atoms are released precisely where they can have the greatest impact - in the hottest zones of the fire.

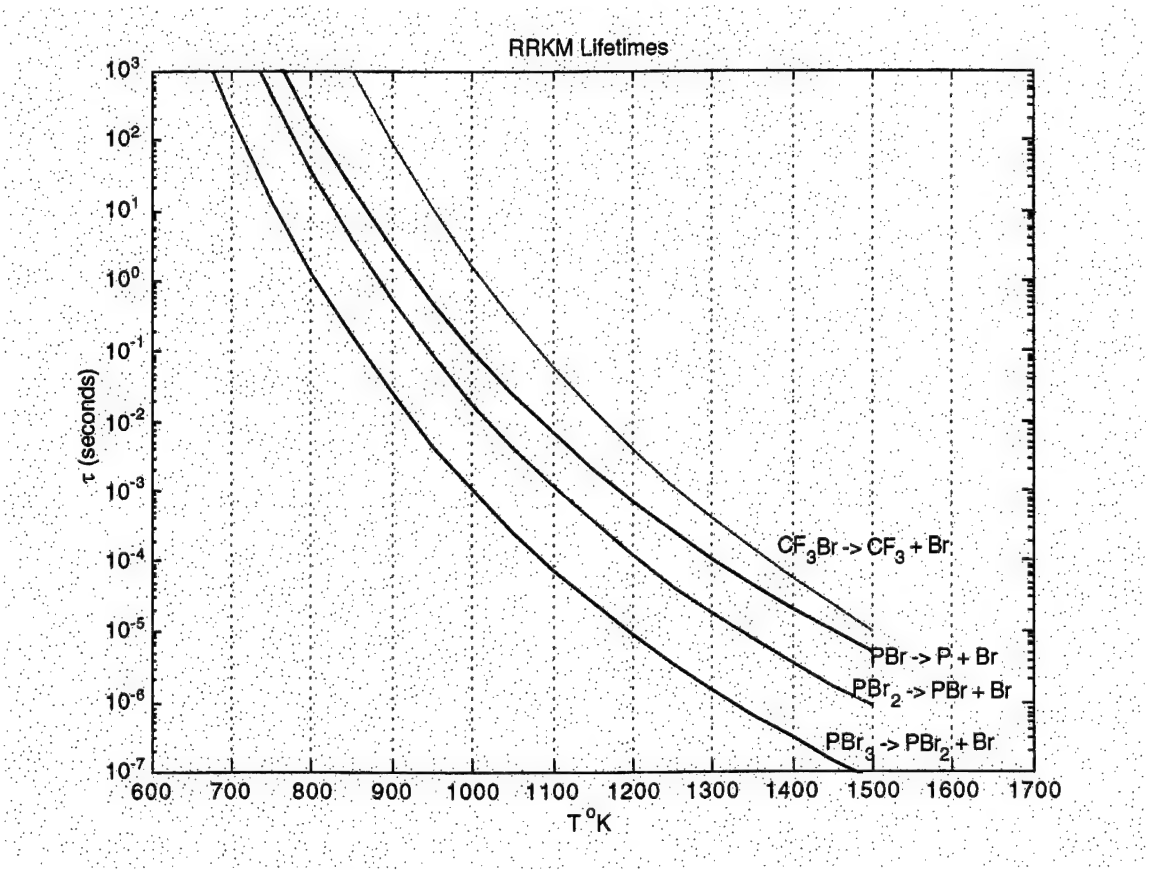

Figure 1. ***Unimolecular lifetimes of PBr_x and CF_3Br as a function of temperature using RRKM theory. Release of bromine atoms by PBr_x is substantially faster than that by Halon 1301.***

Bromine atoms may also be released in the combustion zone by reactions with flame radicals such as the hydrogen atom. Using similar *ab initio* techniques we have also

analyzed the kinetics for reactions of hydrogen atoms with PBr_x, (x=1,2,3) as summarized in Figure 2. The scavenging of H atoms by phosphorous tribromide is competitive with thermal decomposition when the atom number density exceeds about 10^{15} per cubic centimeter; in other words a partial pressure of 0.04 millibar, at flame temperatures of 700-900°C (973-1173°K) such as are measured in our nacelle tests.

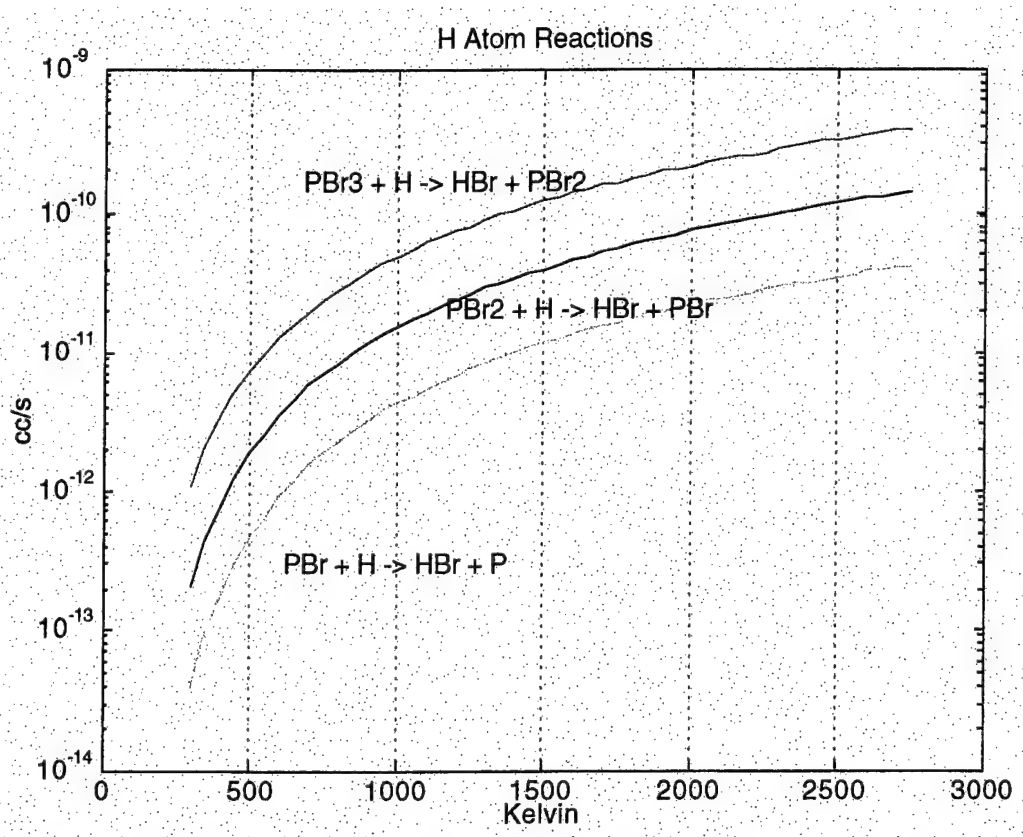

Figure 2. ***Temperature dependent bimolecular rate coefficients (cm^3s^{-1}) for Br abstraction from three PBr_x compounds by hydrogen atoms.***

6. Nacelle Fire Testing

During the phase I SBIR we constructed a small-scale nacelle that completely burned 5 grams per second of kerosene in a 50 kph airstream. Presuming a heat of combustion of 48 kJ/gram for kerosene implies a 240 kilowatt fire. This fire was convincingly extinguished without disrupting the fuel or air flows by injecting as little as one gram (0.3 cc) of PBr_3 into the combustion zone.

We have constructed and tested a full scale nacelle simulator that satisfies the design criteria specified by the FAA Technical Center in Atlantic City for its new nacelle facility and is patterned after the boundary conditions published by WL/FIVS for its nacelle fire test stand. We completely burn 10 grams per second of kerosene in a one-meter long, conical stainless-steel tube that has a 30 cm entrance and a 40 cm exit. The total combustor volume is approximately 96 liters, and the heat release is 480 kilowatts (Figure 3). Fuel sprays exceeding 10 grams per second (0.75 liters per minute) result in uncombusted kerosene dripping from the end of the simulator, so that a power density of approximately 5 kW/liter is the maximum attainable with the present blower, fuel, and geometry. An annular flame holder is centered in the flow provided by a 3000 cfm centrifugal blower, yielding measured flow velocities of 13 meters per second (25 knots) on axis. A pressurized (60 psi) spray of kerosene is directed onto the flame holder and ignited by an automotive flare. Peak temperatures in the combustion zone, which are monitored by thermocouples, are typically 900 to 1000° C (1170-1270° K). All of the experiments were conducted in the Modoc test range at 6000 feet above sea level. Ambient temperatures ranged from -10°C to 25°C.

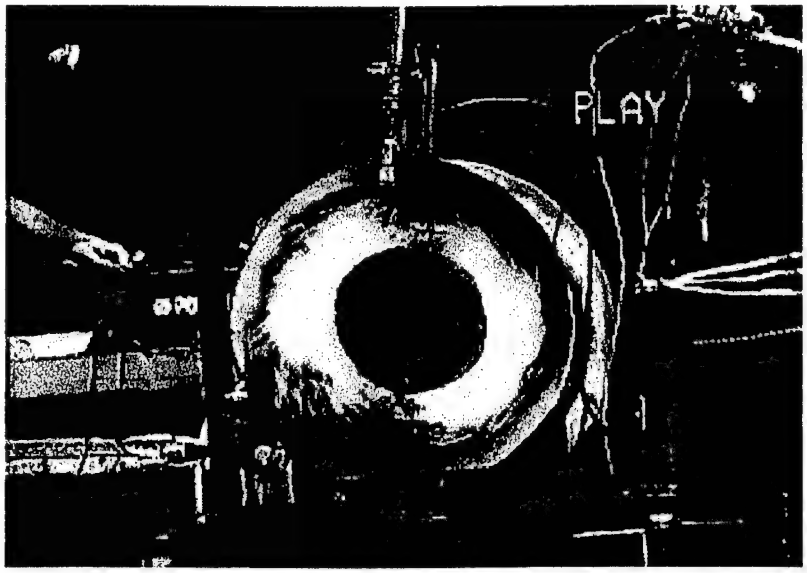

Figure 3 ***End-on view of the nacelle simulator burning 10g/second (12 cc/second) of kerosene in a 13 m/s, 3000 cfm airflow.***

When fuel flow is shut off the fire in the flame-holder continues to burn for up to 10 seconds, as recorded on videotape. (Figure 4). This observation has motivated an innovation in fire suppression by liquids that we call counterflow injection. Agent is typically injected upstream from the combustion zone, leading to a residence time that is roughly equal to the ratio of the combustor length to the flow velocity. Gaseous agents such as Halon 1301 will follow the streamlines in the flow and be forced to diffuse against strong temperature gradients into the flame-holder regions. Aerosols of PBr_3 would also follow the streamlines around flame-holders if they are injected upstream from the fire. However propulsion of the PBr_3 spray against the main flow direction assures penetration of droplets into the flame-holder regions that are shadowed by clutter in the main flow stream. In addition, the inertia of the liquid droplets permits them to cut across streamlines to penetrate regions where diffusion of gaseous agents is constrained. Finally, the residence time of the agent in the fire zone is more than doubled as the spray is first decelerated then reaccelerated by drag forces from the main flow.

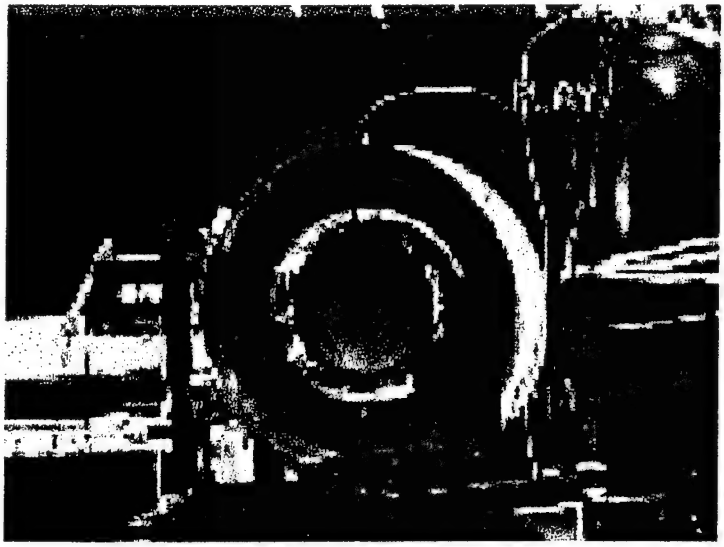

Figure 4 ***Five seconds after fuel flow has been interrupted the fire continues to burn in the flame-holder region. Temperatures up to 800° C have been measured in this region 7 seconds after fuel termination.***

The residence time of an extinguishing agent or combusting fuel droplet in our simulator averages about 80 milliseconds, although stagnation and recirculation around the flame

holder substantially increases this value for some locations in the device. This residence time is short compared to the lifetime of CF_3Br at typical flame temperatures but long compared to the lifetimes for PBr_x summarized in Figures 1 and 2. Thus one expects PBr_3 to be completely dissociated in the flame zone while only a fraction of CF_3Br would release bromine under the same conditions. We confirm the production of Br atoms by qualitative observation of brown Br_2 gas production from the reaction

$$Br + Br + M \rightarrow Br_2 + M$$

at high PBr_3 or $SOBr_2$ loading.

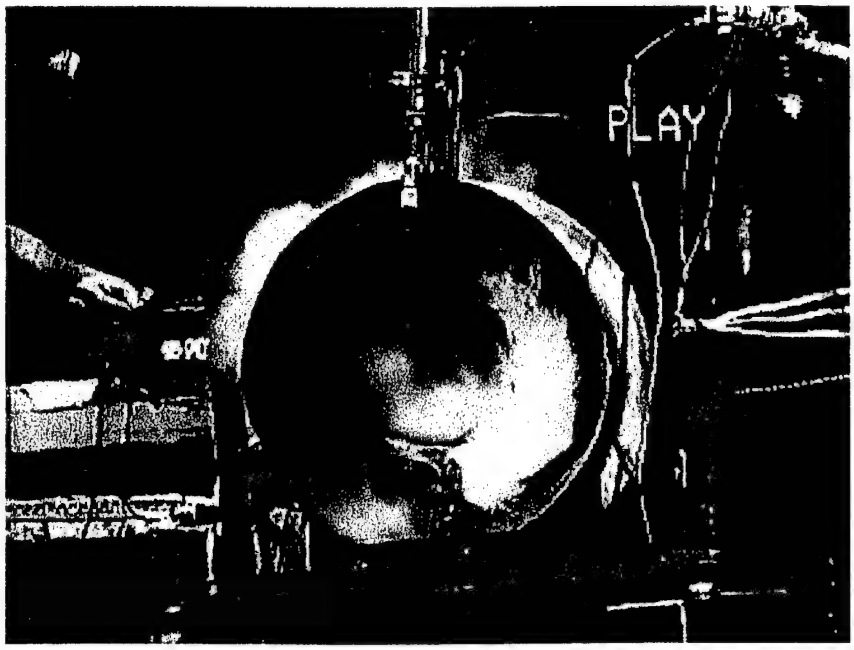

Figure 5. ***First frame of video (within 33 ms) record following injection of 10cc of PBr_3 by about 1 liter atmosphere of nitrogen through a ruptured foil diaphragm.***

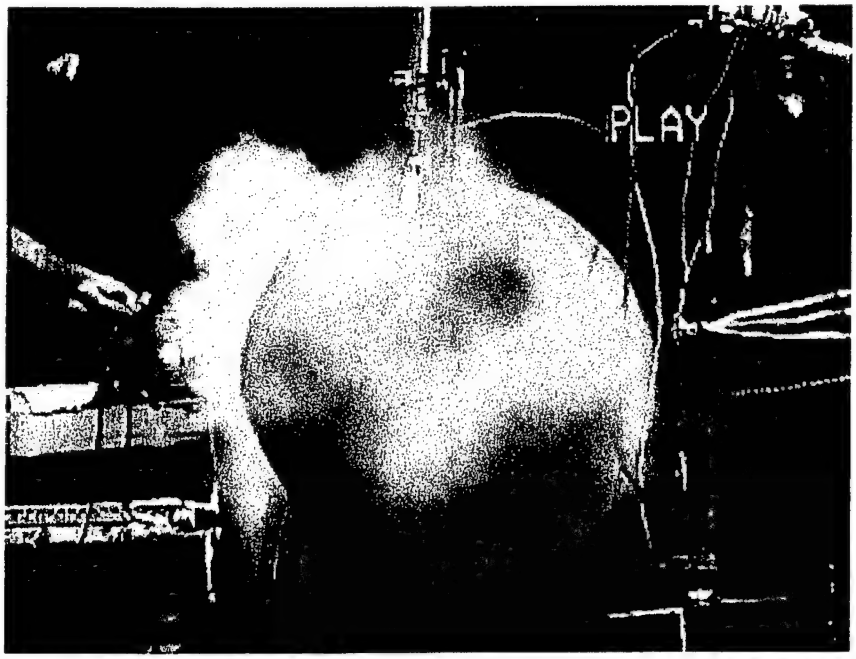

Figure 6. ***Two frames later (100 ms after injection) there is no evidence of flame and copious unburned fuel in the form of kerosene smoke is visible.***

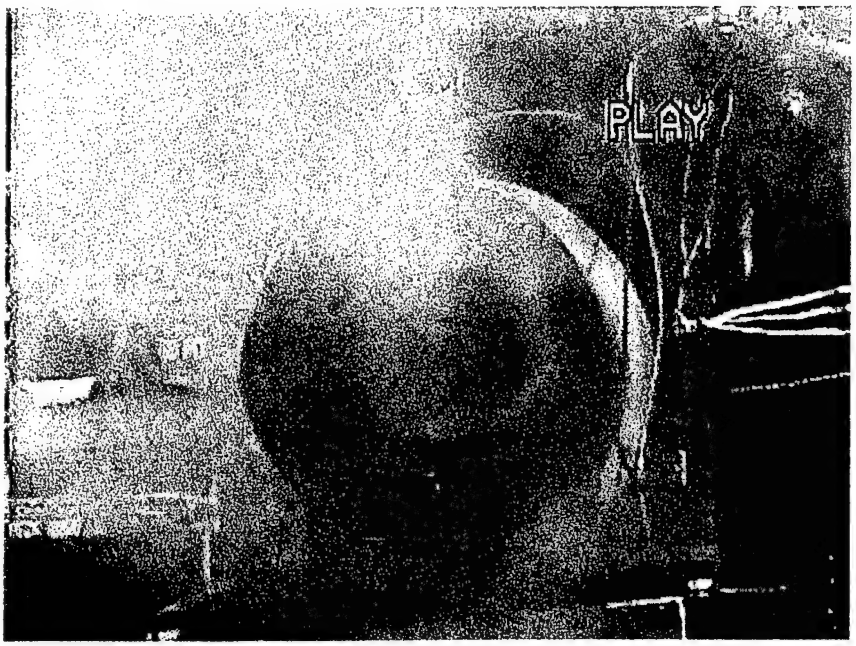

Figure 7. ***Thirty frames (one second) following suppressant addition we see no evidence of combustion in the nacelle, even around the flame holder, despite the fact that fuel continues to flow at 10 grams per second.***

The complete release of available Br from PBr_3 implies that substantially smaller quantities of this agent than of Halons should be required to suppress the 500 kW fire. We have confirmed this hypothesis in many experiments, with typical results shown in Figures 5-7.

The frames shown in these figures employed a ten milliliter (28 gram) aliquot of PBr_3 propelled into the flameholder region by a 1 liter-atmosphere (<1 mg) puff of gaseous nitrogen. Similar results were obtained using liquid or gaseous CO_2 or air as propellants for the liquid. The fire goes out completely, even in the flame-holder region, in less than 100 milliseconds. We were unable to obtain Halon 1301 for comparative testing; however, a fire burning 10cc (8 g/s) of jet fuel per second in the Air Force Nacelle Test Stand run by WL/FIVS reportedly requires several kilograms of Halon 1301 for extinguishment.

The chemical quenching of flames by PBr_3 is orders of magnitude more potent than that of Halons on both mechanistic and empirical grounds. The precise relationship between the amounts of Halon and PBr_3 that are required to suppress specific fires is expected to vary with flame temperature and agent residence time, but it will in all cases result in smaller required masses and volumes of PBr_3 than of Halon 1301, 2402, or 1211.

7. Dry Bay Fire Suppression

A second task of the effort involved suppression of deflagrations such as occur when an incendiary round perforates a fuel tank or avionics dry-bay. A dry-bay test stand was built to examine the application of our approach to fuel spray fires in typical enclosed spaces. The bay is a 2 x 0.3 x 0.5 meter (0.3 cubic meter volume) welded aluminum frame sheathed with galvanized plate in the rear and polycarbonate sheet on the front face to permit video recordings of the fire (Figure 8). A 10 cm diameter exit wound is cut in the polycarbonate and the bay is ventilated by a 140 cubic feet per minute centrifugal blower. 70 cc of kerosene is forcibly sprayed through a foil diaphragm into the chamber, where it is ignited by a gunpowder fuze that is in turn started by a current pulse through a foil layer. The fire is spectacular, filling the bay and propagating 5 meters out of the exit wound. With no suppression the burning on wetted surfaces continues for tens of seconds as seen in Figure 9.

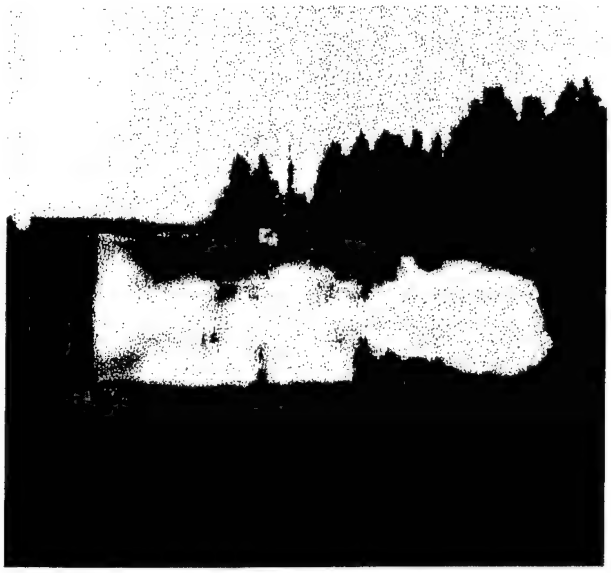

Figure 8. ***Fire in the dry-bay simulator showing 5 meter tongue of flame propelled through the exit wound in the center of the device. Injectors for fuel (center) and extinguishant (right) are also shown.***

Figure 9. ***Six seconds after the initial fire, combustion continues on surfaces that were wetted by fuel. This burning continues both with and without ventilation by the 140 cfm blower.***

The situation is quite different when 10 cc of PBr_3 is injected as shown in Figures 10 through 13. In Figure 10 we see that the fire is fully developed before addition of our Halon replacement. One frame following injection of PBr_3 we see in Figure 12 ample

kerosene smoke and evidence of asymmetry in the combustion zone that we attribute to fire suppression.

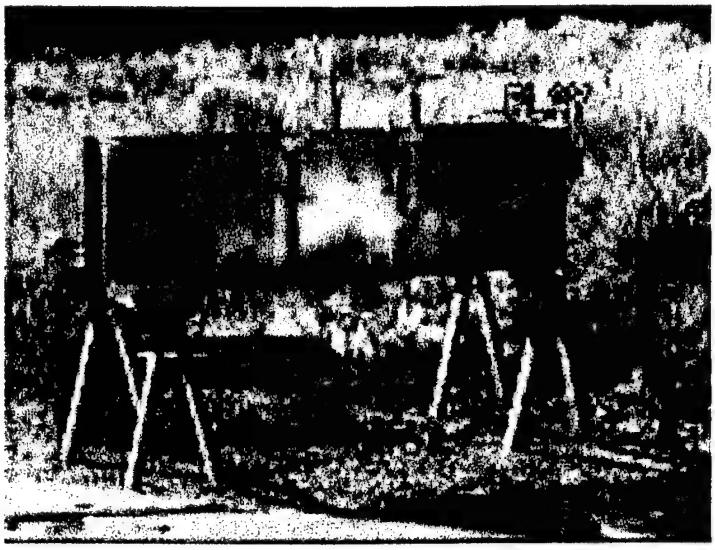

Figure 10. ***This fire has fully developed before we inject 10 cc of PBr_3 into the bay from the cylinder at the right of the figure.***

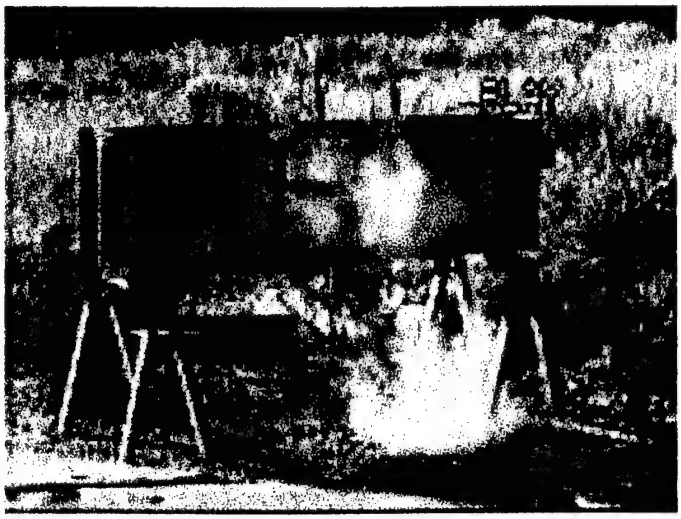

Figure 11. ***One thirtieth of a second (one frame) following injection of PBr_3 we see evidence of suppression in white smoke on the right half of the bay.***

The fire is nearly suppressed two frames later, as seen in Figure 12, and all evidence of combustion is gone within 300 milliseconds of PBr_3 addition (Figure 13). There is no evidence of fire on wetted clutter in the dry bay nor do we see burning on the wetted

surface of the polycarbonate near the exit wound as was unavoidable without suppression . A fire quantitatively similar to this at the WL/FIVS facility requires over 2 kilograms of Halon 1301 for suppression, supporting our mechanistic claim that PBr_3 is more potent than Halon for deflagrations.

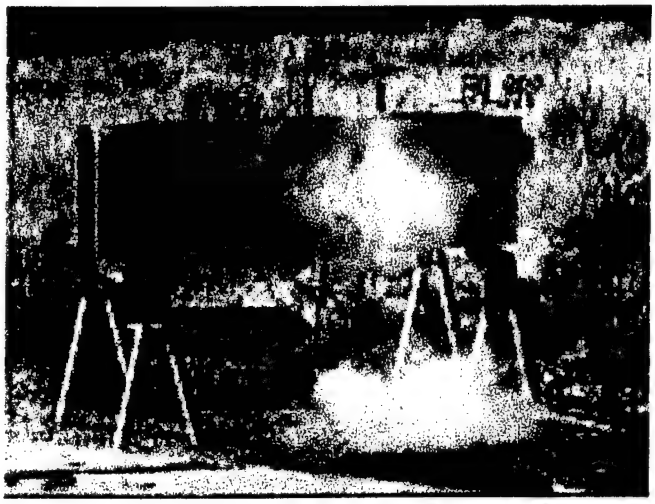

Figure 12. ***Two frame later, or 100 ms following injection of the suppressant, the extinguishment continues.***

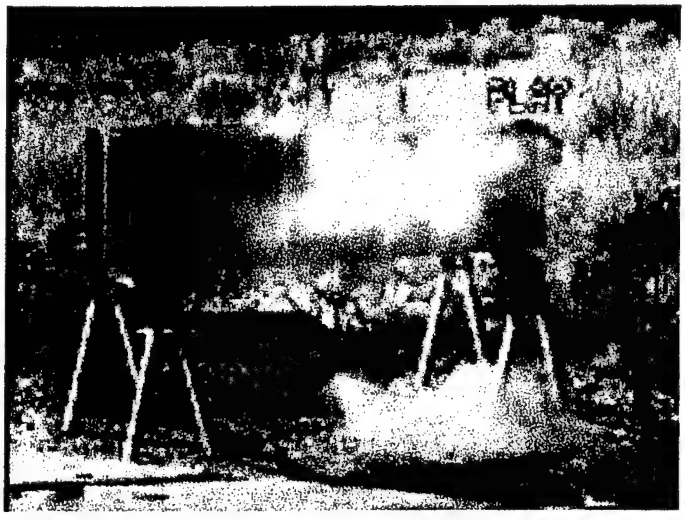

Figure 13. ***The fire is completely suppressed, with no combustion on the wetted surfaces, only ten frames after injection of 10 cc of PBr_3.***

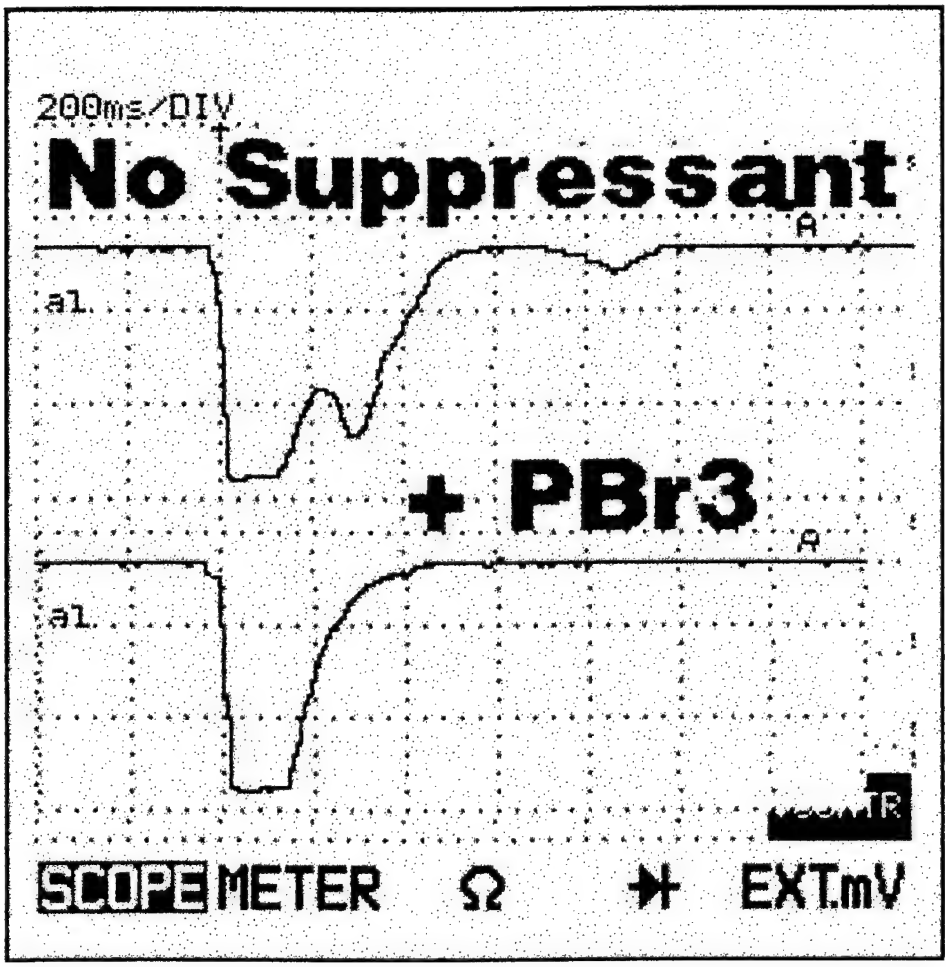

Figure 14. Pressure pulses recorded by a differential transducer for the simulated fuel-tank explosion that results from injection of a 75 cc kerosene spray onto a burning automotive flare in the 0.3 cubic meter dry-bay. A falling signal indicates increasing pressure in the dry-bay.

The most important damage in this type of fire arises from the pressure pulses that accompany deflagration. These pulses are a consequence of hot gases produced by combustion

$$C_xH_y \text{ (kerosene)} + (x+y/2)\ O_2 \text{ ---> } x\ CO_2 + (y/2)\ H_2O$$

as well as heating of air by the combustion products. In the absence of suppressant we observe multiple waves of combustion by light emission (on the videotape) and also by pressure swings recorded with a differential pressure transducer. The main pressure pulse

produced by ignition of the kerosene spray occurs during the first 180 ms of the traces shown in Figure 14. In the absence of suppressant the upper trace shows a pressure fluctuation 350 ms after the leading edge of the initial pulse and a smaller excursion 850 ms after ignition. These are a consequence of secondary deflagration waves in the dry bay. The lower trace, for which PBr_3 was sprayed into the bay after the initial fire, shows no secondary pressure excursions that would result from continued combustion in the dry bay.

8. Theoretical Chemistry

This section summarizes computational studies undertaken by Drs. McKoy and Winstead at the California Institute of Technology to obtain estimates of unimolecular and bimolecular reaction rates involving PBr_3 and its decomposition products. Part A contains structural and energetic information for the species considered. Part B describes and presents the results of the rate coefficient calculations.

8.1. Structure and Energetics of PBr_3 and Related Species

This section reports calculated equilibrium and transition-state structures, and associated energies.

1. Intermediate-Level Calculations

These calculations were carried out in the 6-311G(d) basis at the second-order Moeller-Plesset (MP2) level of approximation as an initial survey. They are superseded by the results in Section 8.2 but may be of interest as a point of comparison.

Table 1: Equilibrium Geometries

Species	Point Group	Structural Parameter	Angstroms / Degrees
PBr_3	C_{3v}	r(P-Br)	2.222
PBr_3	C_{3v}	angle(Br-P-Br)	101.5
PBr_2	C_{2v}	r(P-Br)	2.205
PBr_2	C_{2v}	angle(Br-P-Br)	102.9
PBr	$C_{\infty v}$	r(P-Br)	2.190
Br_2	$D_{\infty h}$	r(Br-Br)	2.295
HBr	$C_{\infty v}$	r(H-Br)	2.699

Table 2. MP2/6-311G(d)//MP2/6-31G(d) Energies

Species	Ground State	Energy (Hartree)
P	^4S	-340.77114
Br	^2P	-2572.45701
PBr	$^3\Sigma$	-2913.30995
PBr_2	$^2B_2$	-5485.85312
PBr_3	$^1A_1$	-8058.39818
Br_2	$^1\Sigma$	-5144.98071
HBr	$^1\Sigma$	-2573.09365

Table 3. MP2/6-311G(d)//MP2/6-31G(d) Dissociation Thresholds

Reactants	Products	Threshold (eV)
PBr_3	PBr_2 + Br	2.39
PBr_3	PBr + Br_2	2.93
PBr_3	PBr + 2Br	4.74
PBr_3	P + 3Br	6.97
PBr_2	PBr + Br	2.76
PBr_2	P + Br_2	2.76
PBr_2	P + 2Br	4.57
PBr	P + Br	2.23

8.2 Methodology for structure and energetics

The equilibrium geometries and electronic energies were computed using a variant of the "Gaussian-2" (G2) procedure of Curtiss et al. [L. A. Curtiss, K. Raghavachari, G. W.Trucks, and J. A. Pople, J. Chem. Phys. 94, 7221 (1991); L. A. Curtiss, M. P. McGrath, J.-P. Blaudeau, N. E. Davis, R. C. Binning, and L.Radom, J. Chem. Phys. 6104 (1995)] with effective core potentials [M. N. Glukhovtsev, A. Pross, M. P. McGrath, and L. Radom, J. Chem. Phys. 103, 1878 (1995); erratum, J. Chem. Phys. 104, 3407 (1996)]. The present work follows the G2[ECP(HW)] methodology of Glukhovtsev et al. with two minor changes: First, we use unscaled MP2/6-31G(d) vibrational frequencies, rather than scaled Hartree-Fock frequencies, to compute zero-point energies and vibrational partition functions. Second, we do not exclude the "core-

antibonding" virtual orbitals in our higher-level calculations. Both of these changes represent (minor) improvements on the canonical procedure.

For the H+HBr reaction system, we carried out directly the type of calculation that the G2 procedure aims to approximate; thus, for H_2, HBr, H, and Br, we performed QCISD(T)/6-311+G(3df,2p)//MP2/6-311+G(d,p) calculations and added the "higher-level corrections" of Gaussian-1 and -2 theory, the MP2/6-311+G(d,p) zero-point energy, and (where needed) a spin-orbit correction, to obtain G2-or-better results without the usual series of calculations.

Where a barrier exists in the adiabatic electronic potential along the dissociation coordinate, the treatment of transition states is straightforward: structures, vibrational frequencies, and energetics are computed via the same procedure used for equilibrium geometries--i.e., G2[ECP(HW)] (except for H+HBr, as noted above). However, unimolecular reactions such as PBr_3 <--> PBr_2 + Br typically do not have barriers in the dissociation coordinate, and the definition of the transition state becomes more ambiguous. In these cases we chose the transition state as a point where (1) the gradient of the electronic potential energy was small, (2) the electronic energy was close to (but typically still below) the asymptotic total energy of the fragments, and (3) the internal coordinates of the fragments were close to their values at infinite separation. The intent was to employ a structure whose partition function would approximate that of the "true" transition state (as might be defined by variational transition state theory, for example).

Because the MP2 method used for geometry searches within the G2 procedure works poorly at nearly-dissociated geometries, we instead used multiconfiguration SCF (MCSCF) to obtain these approximate "loose" transition-state structures and vibrational frequencies. For consistency, equivalent MCSCF calculations were used to obtain the structure and

frequencies (and thus the partition functions) for the corresponding equilibrium geometries. However, the difference of MCSCF energies did not give a sensible activation energy; in these cases we therefore took the activation to be the dissociation energy, as computed at the G2[ECP(HW)] level.

Table 4. MP2/6-31G(d)[ECP(HW)] Structures used in G2 calculations

Species	Symmetry	Structural Parameters Angstroms and Degrees
PBr	$C_{\infty v}$	r(P-Br) = 2.2094
PBr_2	C_{2v}	r(P-Br) = 2.2256 ∠(Br-P-Br) = 103.387
PBr_3	C_{3v}	r(P-Br) = 2.2455 ∠(Br-P-Br) = 101.590
CF_3	C_{3v}	r(C-F) = 1.3272 ∠(F-C-F) = 111.199
CF_3Br	C_{3v}	r(C-Br) = 1.9251 r(C-F) = 1.3358 ∠(F-C-Br) = 110.182
HBr	$C_{\infty v}$	r(H-Br) = 1.4357
HOBr	C_s	r(O-H) = 0.9791 r(O-Br) = 1.8705 ∠(H-O-Br) = 102.145
OH	$C_{\infty v}$	
PBrH (#)	$C_{\infty v}$	r(P-Br) = 2.3591 r(Br-H) = 1.8508
PBr_2H(#)	C_s	r(Br-H) = 1.8472 r(Br-P) = 2.3673 r(Br'-P) = 2.2124 ∠(H-Br-P) = 177.72 ∠(Br-P-Br') = 103.23
PBr_3H (#)	C_s	r(Br-H) = 1.8585 r(Br-P) = 2.3748 r(Br'-P) = 2.2330 ∠(H-Br-P) = 175.052 ∠(Br-P-Br') = 101.416 dihedral(HBrP/BrPBr) = +/-127.377
PBrOH(#)	C_s	r(P-Br) = 2.4477 r(Br-O) = 1.9715 r(O-H) = 0.9777 ∠(P-Br-O) = 173.06 ∠(Br-O-H) = 102.11

Transition state.

Table 5. G2(ECP/HW) Energies

Species	State	Energy (Hartree)	Previous work
P	^4S	-340.81821	-340.81822 [Curtiss]
Br	^2P	-13.10831	-13.10825 [Glukhovtsev]
PBr	$^3\Sigma^-$	-354.02011	
PBr_2	$^2B_2$	-367.22265	
PBr_3	$^1A_1$	-380.42375	
Br_2	$^1\Sigma_+$	-26.28248	-26.28252 [Glukhovtsev]
CF_3	$^2A_1$	-337.22427	
CF_3Br (*)	$^1A_1$	-350.44336	
HBr	$^1\Sigma_+$	-13.74352	
HOBr	$^1A'$	-88.83052	
OH	$^2\Pi$	-75.64391	
PBrH (#)	$^4\Sigma^-$	-354.51493	
PBr_2H (#)	$^3A''$	-367.71817	
PBr_3H (#)	$^2A'$	-380.92005	
PBrOH (#)	$^4A'$	-429.64524	

* Estimated. The MP4/6-311G(2df,p) energy run could not be completed, so its contribution was estimated by adding to the MP2/6-311G(2df,p) energy the sum of the changes [E(MP4)-E(MP2)] for CF3 and Br.
# Transition state.

Table 6. H+HBr System: MP2/6-311+G(d,p) Structures

Species	Symmetry	Angstroms
HBr	$C_{\infty v}$	r(H-Br) = 1.4082
H2	$D_{\infty h}$	r(H-H) = 0.7385
H-H-Br	$C_{\infty v}$	r(H-Br) = 1.5012
		r(H-H) = 1.1059

Table 7. H+HBr System: Better-than-G2 Energies

Species	State	Energy (Hartree)
H	Singlet ^1S	-0.50000
Br	Doublet ^2P	-2572.69546
H2	$^1\Sigma_g^+$	-1.16549
HBr	$^1\Sigma_g$	-2573.33138
H-H-Br	$^2\Sigma_+$	-2573.82938

8.3 Rates

Thermal reaction rates k(T) were computed from the RRKM expression,

$$k(T) = kB * T * Q^{\#}(T) * \exp(-EA/(kB*T))/ (h * Q(T))$$

where T is temperature, kB Boltzmann's constant, h Planck's constant, EA the activation energy, and Q and $Q^{\#}$ the partition functions of the initial and transition states, respectively. The partition functions were evaluated as products of translational, rotational, vibrational, and electronic factors, employing, respectively, the ideal-gas, rigid-rotor, harmonic-oscillator, and Russell-Saunders approximations, together with computed structural and vibrational information. Partition functions also included a structural degeneracy factor. EA was the difference of the transition-state and initial-state G2 energies except as discussed in the preceding section.

Rates for the H+HBr reaction have been measured by Seakins and Pilling [J. Phys. Chem. 95, 9878 (1991)] and by Talukdar et al. [Int. J. Chem. Kin. 24, 973 (1992)]. The present calculations are in reasonably good agreement with these experiments. For the H + PBr_3 abstraction reaction, a rate has been measured by Jourdain et al. [J. Phys. Chem. 86, 4170 (1982)]; our computed rate is considerably smaller in this case. We are not aware of measurements for the other reactions studied.

Data used in evaluating Q(T) and EA follow in Tables 8 to 12. The rates themselves are plotted in Figure 1 and are available in digital form by request to carl@schwinger.caltech.edu or haalanpd@rmi.net..

Table 8. MP2/6-31G(d)[ECP(HW)] Partition-Function Data

Species	Electronic Degeneracy	Vibrational Frequencies (1/cm)	Rotational Constants (GHz)	Mass (amu)	Symmetry Number
H	2	--	--	1.00782	1
P	4	--	--	30.97376	1
Br	2	--		78.91834	1
OH	2	3996.9028	580.246915	17.00274	1
HBr	1	2656.1689	246.376615	79.92616	1
HOBr	1	628.0009	590.58934	95.92108	1
		1225.2799	10.17217		
		3703.8593	9.99993		
PBr	3	433.0451	4.611395	109.89210	1
PBr_2	2	132.8515	10.26443	188.81044	2
		416.0070	1.05100		
		423.7270	0.95338		
PBr_3	1	115.1613	1.00092	267.72877	3
		115.1683	1.00092		
		165.4949	0.52928		
		399.2253			
		411.2633			
		411.2654			
PBrH (#)	4	313.00	3.884098	110.89992	1
		313.00			
		425.94			
PBrOH (#)	4	97.7991	313.46601	126.89484	1
		100.4825	2.12868		
		299.6830	2.11432		
		1077.2609			
		3732.3885			
PBr_2H (#)	3	108.4330	9.35750	189.81826	1
		261.7001	0.97223		
		303.5686	0.88072		
		413.1015			
		437.1607			
PBr_3H (#)	2	94.9576	0.99750	268.73660	1
		110.0501	0.91327		
		149.9836	0.50452		
		252.7539			
		255.2047			
		392.5550			
		421.0323			
		432.1635			

---

* Geometry optimization/frequency calculation did not use effective core potential for Br.
# Transition state.

Table 9. Partition-Function Data Used for Unimolecular Dissociations, Including Data for Approximate MCSCF Transition-State Structures

Species	Vibrational Frequencies (1/cm)	Rotational Constants (GHz)	Symmetry Number
PBr	432.2426	4.6545	1
P-Br	--	0.6628	1
PBr_2	126.78 378.02 384.65	9.60857 1.02373 0.92516	2
PBr-Br	11.27 394.21	27.83008 0.23244 0.23051	1
PBr_3	115.0140 115.0210 165.2792 398.8666 410.9229 410.9250	0.99994 0.99994 0.52878	3
PBr_2-Br (*)	18.00 37.26 126.19 401.92 412.42	0.97467 0.30934 0.24150	1
CF_3Br	309.9559 309.9559 357.6680 542.9703 542.9703 760.8033 1117.8769 1273.0383 1273.0383	5.64054 2.08302 2.08302	3
CF_3-Br (*)	37.1314 37.1314 497.8283 497.8284 708.8232 1193.3232 1268.2784 1268.2785	5.50945 0.67695 0.67695	3

(*) MP2 rather than MCSCF results

Table 10. G2[ECP(HW)] Activation Energies for Bimolecular Reactions

Reaction	EA (Hartree)
PBr + H	0.00511
HBr + P	0.04680
PBr + OH	0.01871
HOBr + P	0.00349
PBr_2 + H	0.00449
HBr + PBr	0.04539
PBr_3 + H	0.00370
HBr + PBr_2	0.04613

Table 11. Activation Energies Employed in Unimolecular Reactions

Reactant	EA (Hartree)
PBr	0.09359
PBr_2	0.09423
PBr_3	0.08923
CF_3Br	0.11212

Table 12. Data Employed for H + HBr <--> H2 + Br Rates

(From Better-than-G2 Calculations)

H + HBr Activation Energy = 0.00200 Hartree
H2 + Br Activation Energy = 0.03157 Hartree

Species	Electronic Degeneracy	Vibrational Frequencies (1/cm)	Rotational Constants (GHz)	Mass (amu)	Symmetry Number
H	2			1.00782	1
Br	2			78.91834	1
H_2	1	4531.1104	1838.91268	2.01565	2
HBr	1	2747.327	256.102881	79.92616	1
H-H-Br	2	555.3071	56.723143	80.93399	1

9. Experimental Chemical Kinetics

Selected experimental investigations of chemical kinetics were performed by Dr. Paul Marshall on the University of North Texas and are summarized below.

9.1 UV Detection of PBr_3

PBr_3 has no visible absorption spectrum, and its infrared transitions lie below the long wavelength cut-off of many infrared spectrometers. It does however absorb in the ultra violet and the UV absorption cross sections have been measured by introducing various partial pressures of PBr_3, up to about 2 Torr, the room temperature vapor pressure, into an 8 cm long quartz cell. Data were obtained at wavelengths above 190 nm in a photodiode array spectrometer, and data at 186 nm from the absorption of mercury lamp emission, isolated with monochromator. Linear plots of absorbance versus [PBr_3] verified Beer-Lambert law behavior at absorbances up to 0.3, and yielded the cross sections plotted in Fig. 15. In particular, the cross section at 186 nm was determined to be 1.2 x 10^{-18} cm^2 (base 10). All results were obtained with samples of PBr_3 from Aldrich, with a stated purity of 99.99+%.

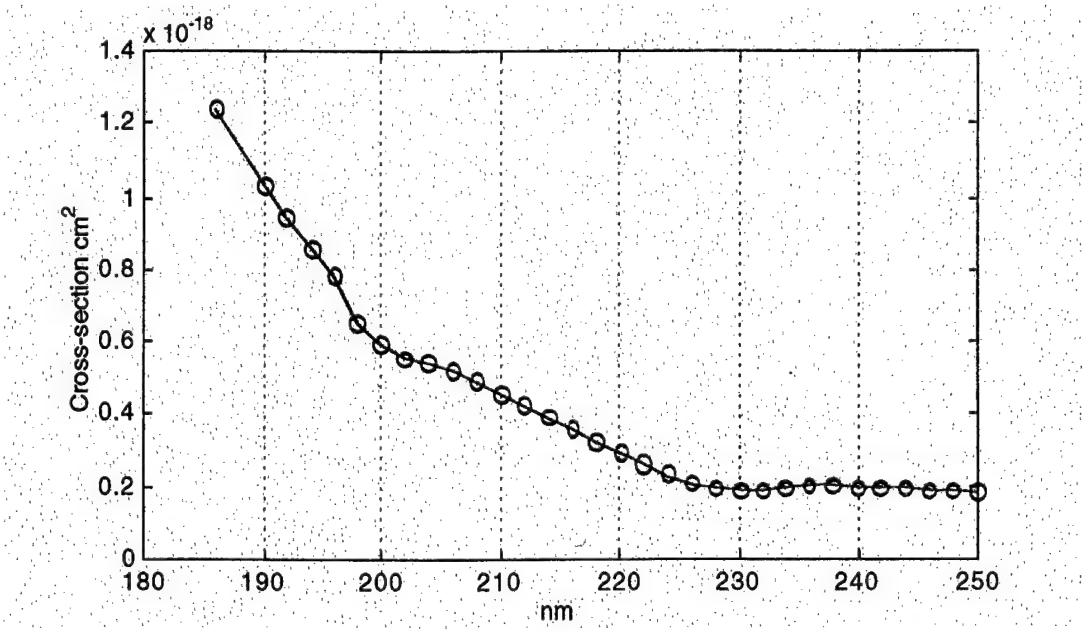

Figure 15. ***Ultraviolet absorption cross-section for PBr_3 vapor.***

9.2 Hydrolysis of PBr_3

Initial experiments were carried out in a fast flow apparatus. Streams of H_2O vapor and PBr_3 vapor, both diluted in argon bath gas, were combined and flowed along a 2 cm diameter reaction tube. The [PBr_3] was monitored downstream of the mixing point, and the reaction time was derived from the known gas flows and the pressure in the reactor (typically around 10 Torr). No change in UV transmittance was observed upon adding water vapor to the PBr_3 stream. Coupled with the residence time of the gases before monitoring, this set an upper limit to rate constant k1 for the bimolecular reaction:

$$PBr_3 + H_2O \text{ --> products} \quad k1 < 6 \times 10^{-17} \text{ cm}^3 \text{ molecule}^{-1} \text{ s}^{-1}.$$

A second set of experiments was based on monitoring a hydrolysis product, HBr, by its infrared absorption near 2610 cm^{-1}. Samples of water and PBr_3 vapors diluted in argon were mixed in a cell within an FTIR spectrometer, and the infrared spectrum was monitored as a function of time. The shortest time scale for these experiments, which required averaging multiple spectral scans, was of the order of a minute, and the reaction appeared to be complete on this time scale. Calibration of the IR absorption with pure HBr samples suggested that approximately 3.7 moles of HBr were formed for each mole of PBr_3 that was hydrolyzed. Allowing for experimental uncertainties, we concluded that gas-phase hydrolysis of PBr_3 breaks all the P-Br bonds, and presumably forms orthophosphorous acid, H_3PO_3.

A third experimental design consisted of a 1 liter bulb, equipped with quartz windows through which 186 nm mercury light was passed (path length about 6 cm). This bulb was filled with about 1 Torr of PBr_3 vapor diluted in argon, and connected to a 3 liter bulb containing 5-15 Torr of water vapor diluted in argon, at a higher pressure. Upon opening the connecting tap, excess water vapor mixed with the PBr_3 and the UV transmittance was

followed on a digital storage oscilloscope. The UV transmittance at 186 nm was seen to decrease, which implies that the UV absorbance of H_3PO_3 plus 3 HBr is greater than that of PBr_3. Preliminary checks showed the absorbance by H_2O under these conditions was negligible. The lifetime (1/e time) for the change in UV transmittance was about 0.2 s. Within the experimental scatter there was no consistent variation with $[H_2O]$, and the conclusion is that the PBr_3 lifetime in these experiments was controlled by the mixing time within the system rather than reaction kinetics. This implies that reaction is fast, and a lower limit of $k1 > 2 \times 10^{-17}$ cm^3 $molecule^{-1}$ s^{-1} was derived.

The two measurements bracket k1, which is estimated as $k1 = (4 +/- 2) \times 10^{-17}$ cm^3 $molecule^{-1}$ s^{-1}. This is fast for a molecule plus molecule reaction. Even in a dry atmosphere containing only 1 Torr partial pressure of water vapor, the atmospheric lifetime of PBr_3 will be of the order of 1 second.

9.3 Unimolecular Decomposition

Initial experiments involved passage of PBr_3 vapor through a heated quartz tube, followed by monitoring of the UV absorbance of the cooled effluent at 186 nm. No changes in the absorbance were seen even at temperatures up to 800 K. A possible interpretation is that either PBr_3 decomposed but was reformed in the cooler observation zone, or that the decomposition products have a similar absorbance to PBr_3 at 186 nm.

Preliminary observations of the UV absorbance directly in the heated zone indicate that with a residence time of 7 s, at 450° K PBr_3 survives while at 650° K PBr_3 is destroyed. This latter result implies an effective first order decomposition rate constant of at least 10 s^{-1} at 650° K, which is substantially faster than the theoretical estimates shown in Figure 1, but qualitatively confirms the labile nature of the P-Br bond in PBr_3.

9.4 Reactions with Radicals

The apparatus consisted of a six-way quartz (or stainless steel) reactor constructed of 2.5 cm (outer diameter) tubing and side arms approximately 15 cm long, with a total volume of 300 cm^3. The intersection region of the side arms defines the reaction zone, where transient species are generated photolytically and detected by resonance fluorescence. Pulsed UV radiation enters the reactor through one port, resonance radiation through another at right angles, and fluorescence exits via a third mutually perpendicular sidearm. The other three sidearms are used as a gas inlet and outlet, and as a port to hold a thermocouple.

Radicals (Br, H and O atoms) were generated by pulsed photolysis of precursor molecules (CH_2Br_2, NH_3 and N_2O, SO_2 and O_2 respectively). In the initial work a flashlamp was employed, but for the final experiments an excimer laser was employed to generate photolysis pulses at 193 nm. The radicals were generated in the presence of excess PBr_3, and for example in the case of the reaction with ground state atomic oxygen,

$$O + PBr_3 \text{ --> products}$$

with bimolecular rate constant k2, the concentration of O atoms after generation is given by

$$d[O]/dt = -k2[O][PBr_3] - k_{diff}[O] = -kps1[O]$$

where k_{diff} accounts for diffusional loss of O atoms to the walls of the reactor. The initial [O] varied between (1-5) x 10^{11} molecule cm^{-3}, while $[PBr_3]$ was typically up to 10^{14} molecule cm^{-3}. Thus $[PBr_3] >> [O]$ and was essentially constant, so that pseudo-first-order conditions held. The effective pseudo-first-order rate constant kps1 was obtained from fitting to the exponential decay of [O], and k2 was obtained as the slope of a linear plot of kps1 versus $[PBr_3]$.

The radical concentration in the zone at the center of the reactor was monitored as a function of time over a few milliseconds, with microsecond resolution, by resonance fluorescence spectroscopy. Atomic resonance radiation in the vacuum UV, about 131 nm for O-atom detection, was generated by a microwave-powered discharge lamp and focused via magnesium fluoride optics. The fluorescence is proportional to the radical concentration. The fluorescence was detected with a solar-blind photomultiplier tube operated in the pulse counting mode, interfaced to a computer-controlled multichannel scaler to obtain photon counts as a function of time, and thus the O atom concentration as a function of time. Typically, results from 100-200 decays were averaged to reduce random noise in the signals.

Initial experiments on reaction 2 showed that the k2 values obtained were independent of the O-atom precursor employed, O_2, N_2O or SO_2; SO_2 was used in the final experiments. The results were also independent of the photolysis pulse energy, and thus of the initial radical concentration, indicating that reaction 2 had been successfully isolated from any interference by secondary chemistry involving photolysis or reaction products. Initial experiments did find a consistent variation of the apparent k2 with the residence time of PBr_3 in the reactor system. Similar effects persisted with both quartz and steel reactors, with both steel and polypropylene gas connections, and whether the PBr_3 and O-atom precursor were mixed in the reactor or earlier in the gas-handling system. Ultimately, after several weeks of passivation in the quartz reactor, the k2 values became independent of residence time at room temperature. The results were similar to those obtained by extrapolating the earlier data to zero residence time in the reactor. We speculate that PBr_3 easily absorbs onto surfaces and/or reacts there, perhaps with traces of moisture, and this can interfere with kinetics measurements because the high reactivity of PBr_3 requires the use of very low gas phase concentrations. Even a small amount of surface loss can therefore cause a significant change in the gas phase concentration when this is initially

low. For this reason sets of experiments carried out on the reactions of PBr_3 with H atoms and Br atoms before the significance of these surface losses were appreciated are unreliable, and are not reported here. They will be repeated. At temperatures above room temperature it proved impossible to eliminate the residence time dependence of k2, and thus these measurements were extrapolated to zero residence time.

Sets of experiments were carried out at 298, 388 and 487 °K. The temperature dependence is weak and not significantly different from zero, given an estimated factor of 2 uncertainty in the k2 values derived by extrapolation to zero reaction time. The best fit Arrhenius expression is

$$k2 = 8 \times 10^{-11} \exp(-4 \text{ kJ mol}^{-1}/RT) \text{ cm}^3 \text{ molecule}^{-1} \text{ s}^{-1}.$$

10. Toxicology of PBr_3

Management Technology Environmental, the on-site support contractor for the Tri-Service toxicology laboratory AL/OET, performed acute toxicity evaluations with Daphnia and Fathead minnows as well as genotoxicity using Salmonella (the Ames test) under subcontract.

The EC50 for Daphnia exposed for 48 hours is 22.6 mg/liter (18.2 - 27.9 mg/liter range) with no observable effect at concentrations below 6.25 mg/liter. The LC50 dose for 96 hour exposure of fathead minnows is 71 mg/liter (50-100 mg/liter range) with no observable effect on the organisms at doses below 25 mg/liter. For these tests materials that have no toxicity at doses of 100mg/liter are considered to be non-toxic. In the spectrum of known materials PBr_3 is nearly non-toxic to aquatic organisms.

No microsome mutagenesis was observed in the genotoxicity tests for either base-pair substitution (TA 100, TA 1535) or frame-shift (TA 98, TA 1537) mutations at doses to 5 mg per plate either with or without buffering to pH 6.8.

The full subcontractor reports describing the aquatic and genotoxicity data are available on request.

In an independent study scientists at the U.S. Air Force Armstrong Laboratory performed acute and subchronic toxicity tests of PBr_3. The report is authored by Robin Wolfe, Marcia Feldman, David Ellis, Harry Leahy, Carlyle Flemming, Darol Dodd, and Jeffery Eggers and is entitled Acute and Subchronic Toxicity Evaluations of the Halon Replacement Candidate Phosphorous Tribromide. The complete technical report of their investigation has been published and is available through the National Technical Information Service. (NTIS Order Number: AD-A329 386/7INZ. To order, call the NTIS sales desk at 1-800-553-6847. This product may also be ordered by fax at (703) 321-8547, or by e-mail at orders@ntis.fedworld.gov. NTIS is located at 5285 Port Royal Road, Springfield, VA 22161. Price: $21.50) The report will also be available on the internet at the Armstrong Laboratory website: http://voyager.wpafb.af.mil/frames/publications.html.

11. Risk Assessment

The toxicity data were then combined with an exposure model to assess the risk associated with use of PBr_3 as a fire suppressant in aviation applications. The risk assessment, which was performed by Dr. Mattie of Armstrong Laboratory, was presented at the Conference on Issues and Applications in Toxicology and Risk Assessment that was held from 27-30 April 1998 at Wright-Patterson AFB, Ohio. This report, for which HRE provided chemical kinetic and transport data, is reproduced in section 11.2, below.

11.1 Transport properties of PBr_3 vapor

The vapor pressure of PBr_3 is 2.25 Torr (2.96 mbar) at 20°C. Plots of the vapor pressure near room temperature and up to the atmospheric pressure boiling point quantify the low volatility of PBr_3 liquid.

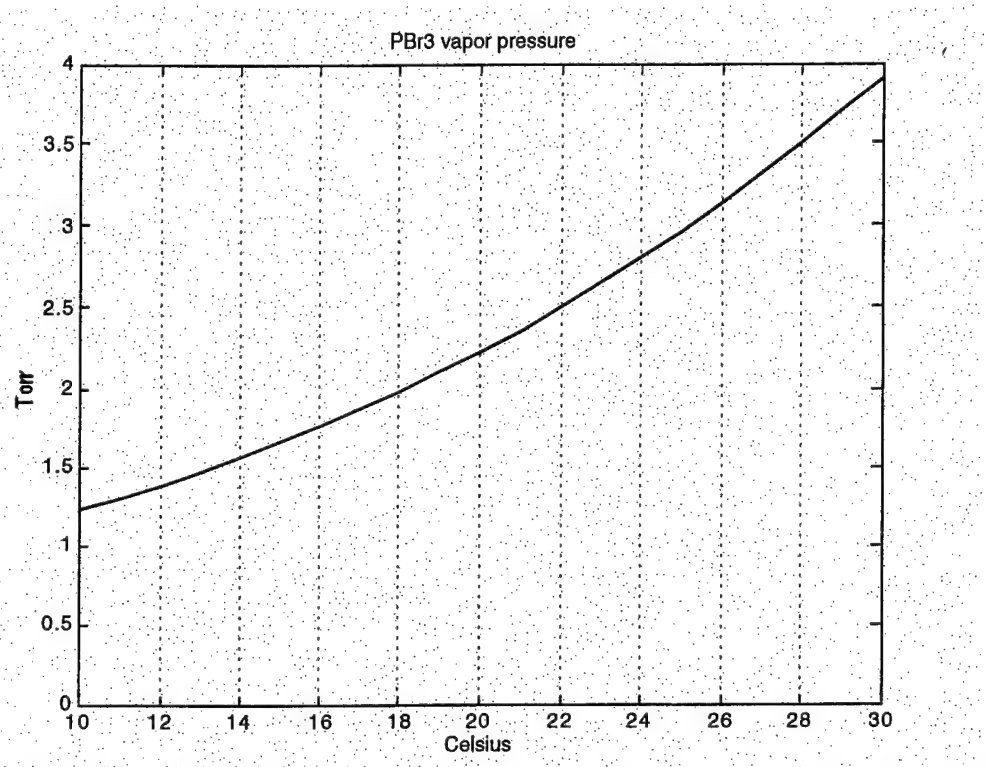

Figure 16*PBr_3 vapor pressure (Torr) between 10 and 30 Celsius on a linear scale. The room-temperature vapor pressure is 2.25 Torr.*

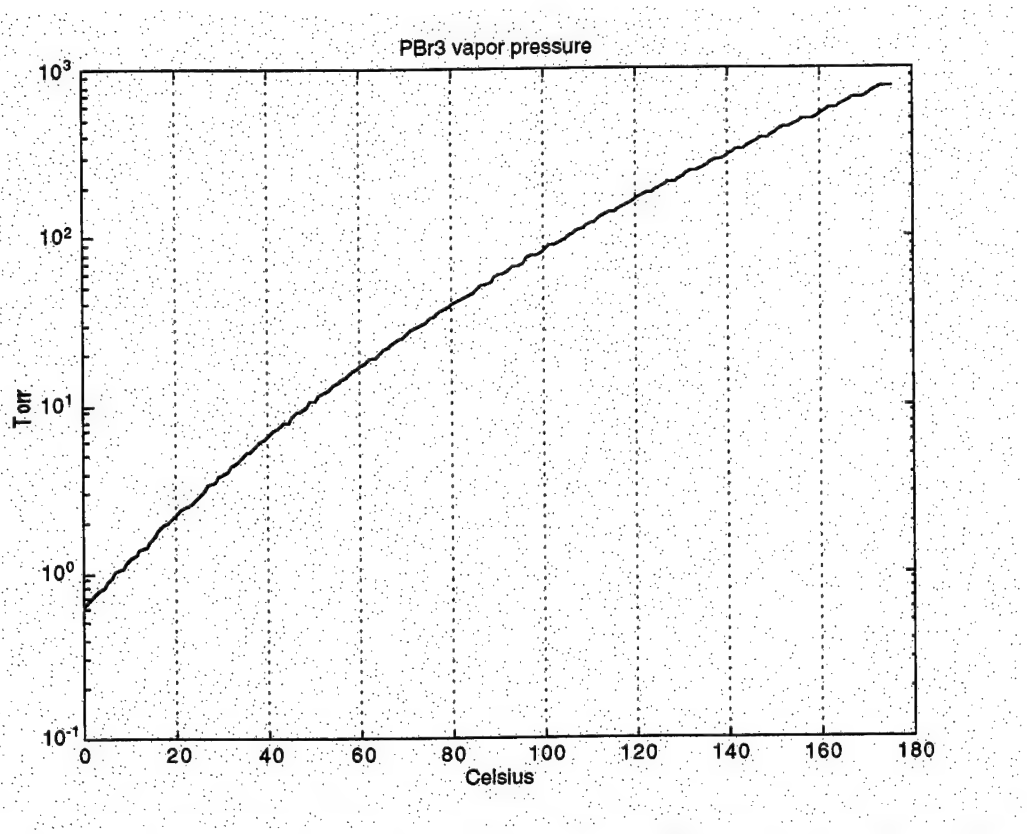

Figure 17*Vapor pressure (Torr) of PBr_3 between 0°C and its boiling point at atmospheric pressure.*

As it slowly diffuses from a puddle or spill PBr_3 vapor reacts rapidly with atmospheric moisture according to the reaction:

$$PBr_3 + 3H_2O \text{ --> } 3\ HBr + H_3PO_3$$

whose measured rate is $4 \times 10^{-17} cm^2 s^{-1}$. To compute the hydrolysis rate one needs to know the amount of water in air in molecules per cubic centimeter. At room temperature this quantity is expressed as the product of the relative humidity and the saturated vapor pressure of water, which is 17.5 Torr or 6×10^{18} molecules per cubic centimeter. Collecting the constants and taking the reciprocal of the rate coefficient gives a lifetime for PBr_3 in air as

$$\tau = \frac{1}{24.7(RH)} \text{seconds}$$

where RH is the relative humidity, expressed as a fraction. At 50% relative humidity RH=0.5 and the hydrolysis lifetime is 81 milliseconds. At 5% relative humidity this lifetime increases to 810 milliseconds, and at 100 % RH the lifetime is 41 milliseconds.

An additional constraint on occupational exposure to PBr_3 vapor comes from the slow diffusion of this heavy gas. Using the Chapman-Enskogg approximation we estimate a diffusion constant at atmospheric pressure and room temperature is 0.03 cm^2s^{-1}. The diffusion velocity is equal to this constant times the concentration gradient for the material. Alternatively, one can define a time constant in seconds for diffusion in a fundamental mode as

$$\tau_d = \frac{\Lambda^2}{D} = 3.2\Lambda^2$$

where Λ is a characteristic dimension for the volume under consideration; it is close to the diameter of a cylinder, the radius of a sphere, or the edge of a cube. Since these dimensions are between tens and thousands of centimeters for most plausible risk scenarios we see that the diffusive transport of this agent is very slow compared to the rate at which it reacts with ambient water vapor *(vide infra)*. The slow diffusion of PBr_3 vapor implies that its transport will be primarily convective, so that information or measurements of ventilation rates may be used to quantify exposures for scenarios other than those described below.

The slow diffusion of PBr_3 also constrains the evaporation rate of a liquid puddle or spill. A boundary layer of the heavy vapor forms over the liquid surface; diffusion through this boundary layer constrains the evaporation rate, so that the real mass transfer depends on the convective boundary conditions. Mass transfer is also affected by diffusion of water vapor from the atmosphere into the puddle. This water reacts with PBr_3 to produce non-volatile H_3PO_3 and HBr gas, some of which may remain dissolved in the liquid. In order to support the risk assessment we therefore made experimental measurements of the

evaporation rate from a puddle of PBr_3. We find a mass transfer rate of 7.6 $\mu g/cm^2 s$ at room temperature with moderate ventilation, as described below in section 11.2.2 and Figure 18.

11.2 Risk Assessment for Phosphorous Tribromide.

D R Mattie[1], P D Haaland[2], T R Sterner[3], R E Wolfe[4], D E Dodd[4]. [1]Operational Toxicology, AFRL, WPAFB, OH; [2]Huntington Research and Engineering, San Jose, CA; [3]Operational Technologies Corp., Dayton, OH; [4]ManTech Environmental Technology, Inc., Dayton, OH.

ABSTRACT

Phosphorus tribromide (PBr_3) is being considered by the Department of Defense (DoD) as a possible replacement for Halon 1301. Results of genotoxicity testing using bacterial Salmonella strains indicated PBr_3 is not a mutagen for either frame shift or base-pair substitution tester strains in both buffered and unbuffered solutions. Acute aquatic toxicity testing determined a 96-hour LC_{50} value for fathead minnows at 71 mg/L (25 mg/L NOEC) and a 48-hour EC_{50} value for *Daphnia magna* at 22.6 mg/L (6.25 mg/L NOEC). Application of 10 µL neat PBr_3 to intact skin of an anesthetized NZW rabbit caused edema and necrosis of the treated skin within 10 minutes of dosing. Toxicity was not observed in rats exposed for 4 hr to 0.4 mg/L in an inhalation exposure. Male rats (5/group) were exposed to PBr_3 vapor, 4 hr/d for 5 d, at 0, 0.06, 0.16 and 0.51 mg/L PBr_3; 0.06 mg/L was the NOAEL. Rats (10/sex/group) were exposed to PBr_3 vapor, 4 hr/d, 5 d/wk, for 4 wk at 0, 0.03, 0.1 and 0.3 mg/L; the NOAEL was 0.1 mg/L. Phosphorus tribromide reacts with moisture in the air to produce phosphonic acid and hydrogen bromide gas (HBr). A 10 cc cartridge of PBr_3, tested as a fire suppressant, would react to form an estimated 25 g of HBr. If uniformly distributed in a room 10x10x5 m in size, the maximum HBr concentration would be 0.05 mg/L (50 mg/m^3); if in a 61.5x46.2x14.8 m hangar, it would be 5.9×10^{-4} mg/L (0.59 mg/m^3). Since the exposure limit for HBr is 10 mg/m^3, the maximal hangar concentration would be below the action level, indicating that

an acceptable exposure level during usage on aircraft is possible based on the physical characteristics of PBr_3 and the small amount necessary for fire suppression. Dermal contact with PBr_3 should be avoided due to its corrosive behavior.

11.2.1 Hazard Assessment

Phosphorus tribromide (PBr_3) is being considered by the Department of Defense (DoD) as a possible replacement for Halon 1301. The DoD requires the development of a toxicity profile for replacement candidates of Halons, which includes the results from acute and subchronic toxicity testing. Many potential replacements, including phosphorus tribromide, have not been thoroughly investigated to determine their toxicological properties. The purpose of this report is to summarize the toxicity studies conducted for phosphorus tribromide and to conduct a preliminary risk assessment for this compound. The risk assessment will help determine if phosphorus tribromide (PBr_3) can be used as a Halon replacement compound.

U.S. Air Force tests in a 500,000 BTU/hr test burner demonstrated that PBr_3 is an effective fire extinguishant. The test burner was quenched by only 0.2 mL PBr_3. This volume is several thousand times less than the amounts required of other Halon replacements to suppress fires. New fire extinguishant systems utilizing PBr_3 would occupy less volume, weigh less and require less mechanics than current systems used for U.S. Air Force aircraft and electronic equipment fires. Also, PBr_3 has no ozone depleting potential since it is rapidly hydrolyzed in the troposphere.

Phosphorus tribromide reacts with moisture in the air and at wet surfaces to produce phosphonic acid and hydrogen bromide gas (HBr) according to the following reaction:

$$PBr_3 + 3H_2O \rightarrow 3HBr + H_3PO_3$$

There is limited toxicity information available in the literature for phosphorus tribromide and hydrogen bromide. No acute toxicity information is available for phosphonic acid or hydrobromic acid, the aqueous form of HBr. The combined interaction of these compounds to cause potential health hazards is not known.

In a study of rats exposed to 1300 ppm HBr for 30 minutes, nose-breathing effects were compared to pseudo-mouth-breathing effects. Tissue injury in the nasal region of the respiratory tract was observed, including epithelial and submucosal necrosis. Pseudo-mouth-breathing exposure to HBr caused higher mortality rates and major tissue disruption in the trachea. Observations of the trachea included necrosis of the epithelium, submucosa, glandular tissue and cartilage (Stavert *et al.*, 1991). In a separate study, the rat LC_{50} for one hour was 2858 ppm while the mouse LC_{50} for one hour was 814 ppm (RTECS, 1995a).

Human inhalation of 1300 to 2000 ppm HBr over a period of minutes was reported to be lethal (HSDB, 1995a). A short exposure to 35 ppm caused throat irritation (HSDB, 1995b), while exposure to 5 and 6 ppm for several minutes by 6 human volunteers also resulted in nose (6 out of 6) and throat irritation (1 out of 6) without eye discomfort (6 out of 6) (ACGIH, 1991a; HSDB, 1995c).

An accidental human exposure to PBr_3 and HBr was reported by Kraut and Lilis (1988). While mixing PBr_3, a female laboratory assistant was exposed to PBr_3 and HBr via splashing on the face, chest and hair, and by inhalation of resulting vapors. She remained in the area of the exposure for five to ten minutes. Immediate effects noted were complaint of dry cough, light-headedness and slight congestion of the throat. Over the next two weeks, the subject experienced increasing shortness of breath. Chest x-rays revealed bilateral lobe infiltrates resulting in a diagnosis of chemical pneumonitis. She was allowed to return to work a few months later, though dyspnea on exertion persisted and chest x-ray findings had not yet completely resolved. Recovery was slowed by a number of relapses, apparently due to exposure to other respiratory irritants (Kraut and Lilis, 1988). No

exposure assessment was conducted and attempts to get exposure information were not successful.

Results of genotoxicity testing of bacterial Salmonella strains indicated PBr_3 is not a mutagen. These results were consistent for frame shift and base-pair substitution tester strains in both buffered and unbuffered solutions (ManTech, 1996).

No ecological dose-response levels were reported for HBr. Acute aquatic toxicity tests on fathead minnows (*Pimephales promelas*) and *Daphnia magna* were recently conducted with PBr_3. Fathead minnows (10 per group) were exposed to 0.0, 6.25, 12.5, 25.0, 50.0 or 100.0 mg/L PBr_3 in fresh water (88 mg/L hardness as $CaCO_3$) at 22 ±2 °C. The static tests were performed in replicate and the results were pooled. The 96-hour LC_{50} value for fathead minnow was 71 mg/L (50 - 100 mg/L confidence limit); the no observed effect concentration was 25 mg/L (Aqua Survey, 1996a). These results indicate that an isolated or intermittent exposure to a concentration of PBr_3 equal to 71 mg/L, is likely to cause death to 50 percent of fathead minnows, *Pimephales promelas*. A concentration equal to or less than 25 mg/L is not likely to have an adverse effect. Daphnia (10 per group) were exposed to 0.0, 6.25, 12.5, 25.0, 50.0 or 100.0 mg/L PBr_3 in fresh water (88 mg/L hardness as $CaCO_3$) at 20 ±2 °C. The static tests were performed in replicate and the results were pooled. The 48-hour EC_{50} value for *Daphnia magna* was 22.6 mg/L (18.2 - 27.9 mg/L confidence limit); the no observed effect concentration was 6.25 mg/L (Aqua Survey, 1996b). These results indicate that an isolated or intermittent exposure to a concentration of PBr_3 equal to 22.6 mg/L is likely to cause mortality/immobilization to 50 percent of the Cladoceran *Daphnia magna*, while a concentration equal to or less than 6.25 mg/L is unlikely to have an adverse effect.

Acute and subchronic PBr_3 studies were designed to determine the effects following single, high-concentration exposures which could occur in accidents, as well as repeated, low-concentration exposures which could occur on flight lines or during maintenance.

Application of 10 or 50 μL neat PBr_3 to intact skin of an anesthetized NZW rabbit caused edema and necrosis of the treated skin within 10 minutes of dosing. Microscopic examination confirmed necrosis of the skin and underlying areas, including skeletal muscle of the subcutis. Application of 10 or 50 μL neat PBr_3 to intact skin of an anesthetized NZW rabbit for 30 seconds followed by a water wash for one minute resulted in necrosis of the entire skin, but not the underlying skeletal muscle. An acute 4-hour nose-only exposure of Fischer 344 rats to PBr_3 vapor resulted in mortality at 4.1 mg/L. At 1.5 mg/L, labored breathing, body weight loss, ulceration of anterior nares and rhinitis of the nasal passage were observed. Adverse effects were not observed in rats exposed for 4-hour to 0.4 mg/L. Male rats (5 per group) were exposed to PBr_3 vapor, 4 hours/day for 5 days, at 0, 0.06, 0.16 and 0.51 mg/L PBr_3. There were no signs of adverse effects at the low and mid-exposure levels. Rats in the 0.51 mg/L group had decreased body weights, gross lesions (reddened nares) and microscopic lesions (inflammation of mucosa and ulceration of epithelium in the nares). Rats (10 per sex per group) were exposed to PBr_3 vapor, 4 hours per day, 5 days per week, for 4 weeks at 0, 0.03, 0.1 and 0.3 mg/L. There were no signs of toxic stress, alterations in body weights or changes in organ weights in PBr_3 exposed animals. Minor serum chemistry and hematology effects were observed in the treated animals. Microscopic tissue findings were limited to rats of the 0.3 mg/L group and consisted of mild inflammation of the nasal passages. A concentration of 0.1 mg/L is the no-observable-adverse-effect level (NOAEL) in the 28-day inhalation study (Wolfe *et al.*, 1997).

11.2.2 Exposure Assessment

In order to calculate an inhalation exposure for PBr_3, the following information is needed: vapor pressure (2.25 Torr at 20 °C), molecular weight (270.7), density (2.8 g/cm^3) and evaporation rate of the material as a function of temperature (7.6 $\mu g/cm^2 s$). The

evaporation rate was based on an experiment conducted with a puddle of PBr_3 (4.755 g or 1.66 cc) with a surface area was 15.5 cm^2. The puddle was placed in a moderately ventilated room with a low relative humidity and the mass change was monitored over time at room temperature. The plot below shows the evaporation results, which fit a mass transfer (evaporation) rate of 7.6 micrograms per square centimeter per second. While this value may increase a few fold with more vigorous ventilation it is still four orders of magnitude slower than evaporation into a vacuum. This material (PBr_3) is so dense and its vapor pressure is so low that mass transfer becomes dominated by diffusion.

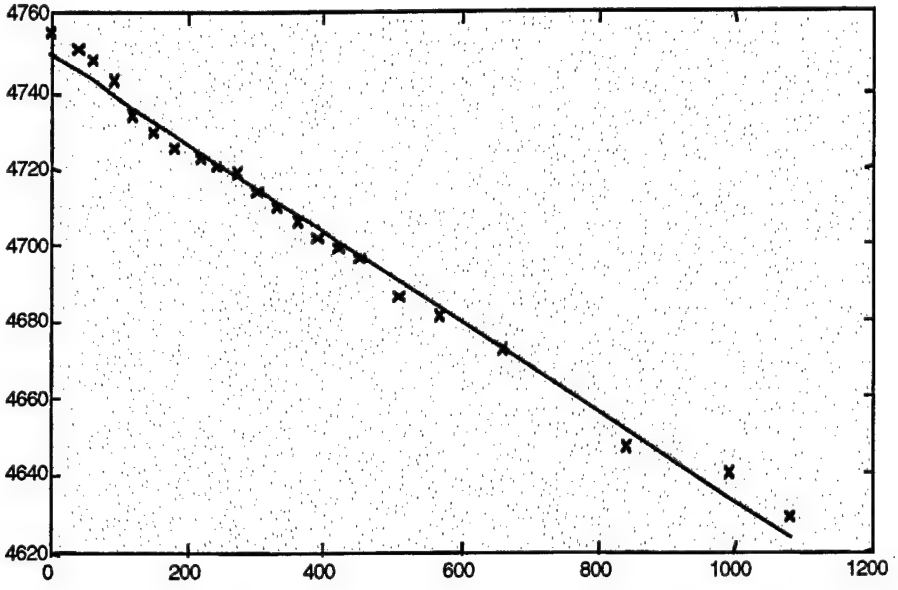

Figure 18. ***Mass of PBr_3 (milligrams) versus time (seconds) in an open weigh boat with a 15.5 cm^2 surface exposed to moderate ventilation at room temperature.***

These numbers can be used to estimate the rate at which PBr_3 is released following a spill or accidental discharge. The density of PBr_3 is greater than aluminum; a spray, stream or aerosol will settle rapidly on the floor in the event of an accidental release.

After evaporation into the air, the material would react rapidly with atmospheric moisture to form HBr and H_3PO_3, according to the reaction:

$$PBr_3 + 3H_2O \rightarrow 3HBr + H_3PO_3.$$

The rate for this reaction is 4 x $10^{-17}cm^2/s$. The hydrolysis rate is based on the amount of water in air in molecules per cubic centimeter. At room temperature this quantity is expressed as the product of the relative humidity and the saturated vapor pressure of water (17.5 Torr or 6 x 10^{18} molecules per cubic centimeter). At 50% relative humidity (RH), the hydrolysis lifetime is 81 milliseconds. At 5% RH the hydrolysis lifetime increases to 810 milliseconds, while at 100% RH it decreases to 41 milliseconds.

The diffusion of PBr_3 vapor is very slow. The slow diffusion of the agent implies that its mixing will be primarily convective and subject to ventilation rates in the work area. Given the high hydrolosis rate even at low RH, PBr_3 would be expected to travel less than 1 cm from the liquid without reacting, under normal work ventilation conditions.

Based on the rapid reaction of liquid PBr_3 with water vapor, it is reasonable to assume that all of the released agent will be quickly converted to HBr and H_3PO_3. H_3PO_3 melts at 74 °C and is very soluble in water (300 grams per 100 cc H_2O), so this material will not be airborne except as an aerosol. HBr, although also very soluble in water (221 grams per 100cc water), is a gas at room temperature (20°C). A conservative assumption for accidental release is, therefore, that all of the PBr_3 is rapidly converted to gaseous HBr and aerosol H_3PO_3, either on contact or by reaction in a zone less than a centimeter from the liquid.

Using this conservative model, the 10 cc PBr_3 cartridge (28.5 grams) that was tested in full scale engine nacelle tests should generate approximately 25.5 grams (0.315 moles or 7.05 liter atmospheres) of HBr. If all of the PBr_3 is converted to HBr and is uniformly distributed in a room 10x10x5 meters in size, the maximum concentration of HBr would be 14.1 ppm. The concentration is inversely proportional to the volume of the room; in a storage closet 2x2x2 meters in size, it would be 881 ppm. These concentrations are upper bounds since the gas will be immobilized as it freely dissolves in the moisture present on surfaces in the room. The rate of surface adsorption of HBr could be easily

quantified by experiment if it is important for modeling smaller rooms. For direct comparison with the inhalation toxicology data, these concentrations can be expressed in mg/liter; 0.05mg/liter (51 mg/m^3) for the small room and 2.96 mg/liter (2,961 mg/m^3) for the closet release.

Although there is no typical hangar size, dimensions of the hangars at Wright-Patterson Air Force Base are approximately 200x50x8 ft or 61.5x46.2x14.8 meters. The total volume of such a hangar is 42,051 m^3. If 25.5 grams of HBr is uniformly distributed in one of these hangars when it is empty, the maximum concentration would be 0.00061 mg/L (6.1x10^{-4}mg/L) or 0.61 µg/L. This would be equal to 0.61 mg/m^3 or 0.18 ppm or 180 ppb. This still is an upper bound because it assumes that all of the agent is sprayed over moist surfaces, through moist air and reacts 100% with the surface water and water vapor without any of it becoming dissolved in water.

11.2.3 Risk Characterization

For HBr exposure limits, the National Institute for Occupational Safety and Health (NIOSH) set a ceiling limit of 10 mg/m^3, the Occupational Safety and Health Administration (OSHA) set a permissible exposure limit (PEL) of 10 mg/m^3 as an 8-hr time weighted average (TWA), and the American Conference of Governmental Industrial Hygienists (ACGIH) set a 10 mg/m^3 threshold limit value (TLV) as a ceiling. The maximal hangar concentration of 0.61 mg/m^3 would be an order of magnitude below the action level for these standards.

The NOAEL for the 28-day inhalation study was 0.1 mg/L for PBr_3. Since PBr_3 reacts to form HBr, the maximum possible concentration of HBr present at the NOAEL was 9.0x10^{-2} mg/L or 90 mg/m^3 (Wolfe *et al.*, 1997). Therefore, the maximal concentration of HBr in the hangar after an accidental discharge of 10 cc PBr_3 would be

two orders of magnitude lower than the concentration of HBr at the NOAEL for PBr_3 in the 28-day study.

The issue then becomes one of using either the standards for HBr or the NOAEL for PBr_3 as exposure limits. Until a standard for PBr_3 is developed and accepted, the standard for HBr will most likely be used by industrial hygientists. Even after a standard is developed for PBr_3, exposure assessment will depend on the measurement of HBr since PBr_3 reacts so quickly with water vapor in the air. PBr_3 would not likely be used in anydrous or dessicated areas in real world situations.

Due to the density of the PBr_3 and slow diffusion rate, it will not travel far after accidental discharge, allowing time for personnel to exit the area. Due to its reactivity, it will convert to HBr which should achieve high concentrations only in small rooms. In the 10x10x5 meter room, the maximum concentration of HBr possible (51 mg/m^3) is still lower (by almost one half) than the concentration of HBr present at the NOAEL for the 28-day PBr_3 study.

The primary hazard arises from direct contact with the skin. The design of the cartridge containing the PBr_3 has to ensure that accidental discharge of the agent cannot occur during handling and installation/removal from engine nacelles and dry bays on air craft. Cartridges should be filled by the supplier and not by maintenance personnel. The use of this agent in occupied spaces is possible but may not be advisable in all cases. How PBr_3 is supplied and its placement in a system can minimize the risks of its use. However, personnel protection should be worn if working directly with PBr_3 or in a position to be directly sprayed at very close range.

11.2.4 Risk Assessment Conclusions

The reactivity of the agent with moisture and the solubility of the acid products in water make elevated airborne concentrations of PBr_3 and HBr extremely unlikely. The concentrations of HBr should be below the action level for exposure standards.

ACKNOWLEDGEMENTS

The animal use described in this study was conducted in accordance with the principles stated in the "Guide for the Care and Use of Laboratory Animals", National Research Council, 1996, and the Animal Welfare Act of 1966, as amended.

11.2.5 Risk Assessment References

1. Stavert, DM, Archuleta, DC, Mehr, MJ, and Lehnert, BE, 1991, Relative Acute Toxicities of Hydrogen Fluoride, Hydrogen Chloride and Hydrogen Bromide in Nose- and Pseudo-Mouth-Breathing Rats, Fund. Appl. Toxicol., 16:635-55.

2. RTECS, 1995a - National Technical Information Service, PB214-270.

3. HSDB, 1995a - BIOFAX Industrial Bio-Test Laboratories, Inc. 17-4/70.

4. HSDB, 1995b - Braker, W and Mossman, A, 1980, Matheson Gas Data Book 6th ed., 372.

5. ACGIH, 1991a, Documentation of the Threshold Limit Values and Biological Exposure Indices, 6th edition, 771-2 (Connecticut State Department of Health, 1955, Unpublished Data, Occupational Health Section, Hartford, CT.).

6. HSDB, 1995c - Clayton, GD, and Clayton, FE (eds.), 1981-82, Patty's Industrial Hygiene and Toxicology: Volume 2A, 2B, 2C: Toxicology 3rd ed., John Wiley & Sons, New York, 2970.

7. Kraut, A. and R. Lilis. 1988. Chemical pneumonitis due to exposure to bromine compounds. *Chest* 94(1):208-210.

8. ManTech Environmental Technology, Inc. 1996. Final Report. Genotoxicity testing of phorphorus tribromide using Salmonella/microsome mutagenesis assay. ManTech Study No. 6053-200 (Task 3.2). March 15 - July 5, 1996.

9. Aqua Survey, Inc. 1996a. Final Report. Phosphorus tribromide - Acute effects on the fathead minnow, *Pimephales promelas*. Study #96-700220-110-4. July 19, 1996.

10. Aqua Survey, Inc. 1996b. Final Report. Phosphorus tribromide - Acute effects on the cladoceran, *Daphnia magna*. Study #96-300120-110-3. July 19,1996.

11. Wolfe, RE, Feldmann, ML, Ellis, DH, Leahy, HF, Flemming, CD, Dodd, DE. 1997, Acute and Subchronic Toxicity Evaluations of the Halon Replacement Candidate Phosphorus Tribromide, AL/OE-TR-1997-0123, Wright-Patterson AFB, OH.

12. Conclusions: Labile Bromine Fire Suppressants

Labile bromine compounds in general and phosphorous tribromide (PBr_3) in particular are promising alternatives to Halon fire suppressants. Their weakly bound bromine atoms are released more quickly and completely in a flame than the bromine atom in Halons, so smaller quantities of agent are required to suppress standard fires. Labile bromine agents are rapidly hydrolyzed in the troposphere and on exposure to moist surfaces, yielding water soluble products. As a result of these rapid reactions the agents have neither global warming nor ozone depletion potentials and are safe to use for normally unoccupied spaces such as engine nacelles or aircraft dry-bays.

The research performed during this contract has developed quantitative understanding of the mechanisms by which Halons suppress fires and a chemical approach with which it may be efficiently replaced without harming the environment. The Air Force has earned a royalty-free license for government use of our US Patent Number 5,626,786, Labile Bromine Fire Suppressants, that was issued on 6 May 1997.